Lentiviral vectors for inducible, transactivator-free advanced therapy medicinal products: Application to CAR-T cells

María Tristán-Manzano,[1,13,14] Noelia Maldonado-Pérez,[2,3,13] Pedro Justicia-Lirio,[1,2,13] Marina Cortijo-Gutierréz,[2] Pablo Tristán-Ramos,[2,12] Carlos Blanco-Benítez,[1,2] Kristina Pavlovic,[2,4] Araceli Aguilar-González,[2,5] Pilar Muñoz,[2,6] Francisco J. Molina-Estevez,[2] Valerie Griesche,[2,7] Juan Antonio Marchal,[8,9,10,11] Sara R. Heras,[2,12] Karim Benabdellah,[2,14] and Francisco Martin[2,3,8,9,14]

[1]LentiStem Biotech, Pfizer-University of Granada-Junta de Andalucía Centre for Genomics and Oncological Research (GENYO), PTS, Avda. de la Ilustración 114, 18016 Granada, Spain; [2]Department of Genomic Medicine, Pfizer-University of Granada-Andalusian Regional Government Centre for Genomics and Oncological Research (GENYO), PTS, Av. de la Ilustración 114, 18016 Granada, Spain; [3]Departamento de Bioquimica y Biología Molecular III e Inmunologia, Facultad de Medicina, Universidad de Granada, PTS Granada – Avenida de la Investigación, 11, 18006 Granada, Spain; [4]Maimonides Institute of Biomedical Research in Cordoba (IMIBIC), Cellular Therapy Unit, Reina Sofía University Hospital, University of Cordoba, Cordoba, Spain; [5]Department of Medicinal & Organic Chemistry and Excellence Research Unit of "Chemistry Applied to Biomedicine and the Environment", Faculty of Pharmacy, University of Granada, Campus de Cartuja s/n, 18071 Granada, Spain; [6]Department de Biología Celular, Facultad de Ciencias, Universidad de Granada, Campus Fuentenueva, 18071 Granada, Spain; [7]DKFZ. German Cancer Research Center, Heidelberg, Baden-Wurtemberg, Germany; [8]Instituto de Investigación Biosanitaria ibs.GRANADA, University Hospitals of Granada – University of Granada, 18016 Granada, Spain; [9]Excellence Research Unit "Modeling Nature" (MNat), University of Granada, 18016 Granada, Spain; [10]Biopathology and Regenerative Medicine Institute (IBIMER), Center for Biomedicinal Research (CIBM), University of Granada, 18016 Granada, Spain; [11]Department of Human Anatomy and Embryology, Faculty of Medicine, University of Granada, Biosanitary Research Institute of Granada (ibs.GRANADA), Granada, Spain; [12]Department de Bioquimica y Biología Molecular II, Faculty of Pharmacy, University of Granada, Campus Universitario de Cartuja, 18071 Granada, Spain

Controlling transgene expression through an externally administered inductor is envisioned as a potent strategy to improve safety and efficacy of gene therapy approaches. Generally, inducible ON systems require a chimeric transcription factor (transactivator) that becomes activated by an inductor, which is not optimal for clinical translation due to their toxicity. We generated previously the first all-in-one, transactivator-free, doxycycline (Dox)-responsive (Lent-On-Plus or LOP) lentiviral vectors (LVs) able to control transgene expression in human stem cells. Here, we have generated new versions of the LOP LVs and have analyzed their applicability for the generation of inducible advanced therapy medicinal products (ATMPs) with special focus on primary human T cells. We have shown that, contrary to all other cell types analyzed, an Is2 insulator must be inserted into the 3′ long terminal repeat of the LOP LVs in order to control transgene expression in human primary T cells. Importantly, inducible primary T cells generated by the LOPIs2 LVs are responsive to ultralow doses of Dox and have no changes in phenotype or function compared with untransduced T cells. We validated the LOPIs2 system by generating inducible CAR-T cells that selectively kill CD19+ cells in the presence of Dox. In summary, we describe here the first transactivator-free, all-one-one system capable of generating Dox-inducible ATMPs.

INTRODUCTION

Gene therapy has demonstrated to be a real alternative for the treatment of several diseases without adequate treatment.[1] However, the therapeutic benefits of several gene therapy strategies are not optimal due to inadequate delivery or to deficient control of the transgenes. Among gene therapy medicinal products, chimeric antigen receptor (CAR)-T cells have become one of the most promising approaches for the treatment of hematological cancers with the approval of six CAR-T medicaments. However, current CAR-T cells quite often present severe side effects (sometimes with fatal outcomes), and they are not efficient for the treatment of solid tumors. Both limitations could be partially solved by generating smart CAR-T cells that could be controlled externally to decide where and when to be active or to secrete potent biomolecules.[2–4]

Different delivery systems (vectors) have been combined with different ways to control transgene expression in order to achieve

an appropriate transgene release at the right time and at the right tissues. Most strategies aim to achieve self-regulation through systems that respond to the cell type (tissue specific) or to endogenous environments, such as stress, inflammation, hypoxia, etc.[5] However, those strategies do not allow clinicians to control the intensity and durability of the therapy based on patient's responses. As an alternative to self-regulated ones, externally controlled systems aim to regulate the expression of the transgene upon administration of an inductor. These systems are designed to induce or block transcription of the gene of interest (GOI) (ON and OFF systems respectively). ON systems are generally the strategies of choice for clinical applications due to their wider intervention opportunities. Most ON systems are based on a chimeric protein (transactivator) able to activate transcription in the presence of a drug.[6] This strategy has been applied to gene therapy strategies based on drugs derived from tetracyclines,[4,7–9] ecdysone,[10,11] mifepristone,[12–17] and rapamycin.[18,19]

Among the existing ON systems, the Tet-On (based on tetracycline-resistance system from bacteria) is the most widely investigated and exploited. In these systems, the transactivator is a chimeric protein composed of the bacterial Tet repressor (TetR) and the activating domain of the viral protein 16 (VP-16) from herpes simplex virus 1 (HSV1). Multiple versions of the initial configuration[20] have rendered Tet-On platforms with high inducibility and sensitivity to doxycycline (Dox) (10 ng/ml).[21–23] However, in the *on* state, the transactivator can bind to *pseudo-TetO* sites (sequences similar to the TetO that are present along the genome), activating the transcription of nearby genes.[24–26] Additionally, the transactivators can be toxic for certain cell types, hindering their application in some primary cells.[25–27] Of note, Smith et al.[28] observed a depletion of antigen-experienced T cells in rtTA-transgenic mice, evidencing the potential difficulties of using these systems to generate clinical-grade inducible CAR-T cells.

In order to avoid the use of transactivators, several Tet-On system based on the original TetR repressor have been developed to regulate siRNA as well as cDNA.[29–35] Compared with rtTA, the potential undesired effects of TetR binding to pseudo-tetO sites is reduced due to the mechanism of action. Indeed, since promoter repression by TetR binding requires a very precise location (+10 bp after the TATA box) to block transcription,[29] it is very unlikely that binding of TetR to pseudo-TetO sites would have a strong effect on gene transcription. On the contrary, binding of rtTA to pseudo-TetO sites will affect promoters at kilobases of distance, promoting their activity. However, these systems still require cloning and/or high TetR concentrations inside the cells in order to achieve tight regulation. In addition, they generally exhibit relatively high leaking and often fail to work properly in relevant primary human cells, thus limiting their applicability as tools to control transgene release in gene therapy.

In 2016, our group developed two TetR-based, all-in-one LVs without (CEET, Lent-On-Plus or LOP) and with (LOPIs2) an Is2 insulator[36] and showed that both systems tightly regulate transgene expression in human stem cells over time.[37] In this work, we analyzed their appli-

cability for the generation of inducible ATMPs, with special focus on primary human T cells. We have shown that, contrary to all other cell types analyzed, only the LOPIs2 LVs can control transgene expression in human primary T cells. Importantly, these cells are responsive to ultralow doses of Dox and have no changes in phenotype or function. We finally validated the LOPIs2 platform by generating *first-in-class*, transactivator-free inducible CAR-T cells.

RESULTS

Behavior of different LVs for the generation of inducible T cells

T cells are the key players in immunotherapy, and several new strategies are oriented to control the expression of different molecules. We therefore tested the behavior of different transactivator-free Tet-On LVs previously developed by our group[35,37] (Figure 1A) to regulate eGFP in T cells. Jurkat (an immortalized human T cell line) and primary human T cells were transduced with the different Tet-On all-in-one LVs, cultured in the presence or absence of Dox for up to 28 or 36 days and analyzed for their titer (Figure S1A) and inducibility (Figure S1B), as shown in Figure 1B. Our data showed that only the two LOP systems (LOP-eGFP and LOPIs2-eGFP LVs), expressing the TetR repressor through the EF1α promoter, efficiently regulated eGFP expression in Jurkat cells (Figures 1C and 1D and Table 1). In addition, almost a complete reversion was observed at 96 h after Dox removal (Figure 1E).

Interestingly, in human primary T cells, only the LOPIs2-eGFP LV (harboring the Is2 insulator) showed a tight control of transgene expression with very low eGFP expression in the absence of Dox (Figure 1F, top-right plot, and Figure 1I) and good inducibility in its presence (Figure 1F, bottom-right plot, and Figures 1G, 1H, and 1J) that are maintained over time (Figure 1G). In addition, the LOPIs2-eGFP was able to respond to very low concentrations of Dox (0.1 ng/ml), an important factor in terms of safety (Figure 1H). Importantly, this system controlled eGFP expression in all the different T cell subsets analyzed (Figures 1I and 1J): T naive/stem cells memory (T_{SCM}: CD45RA+CD62L+), T cell memory (T_{CM}: CD45RA-CD62L+), T effector memory (T_{EM}: CD45RA−CD62L−) and T effector (T_{EFF}: CD45RA+CD62L−). All these data pointed to the LOPIs2-eGFP as the LV of choice to generate CAR-T cells and other gene therapy-ATMPs in which a tight control of the transgene is required. However, there is still room for improvement in term of titers (Figure S1A).

The Is2 insulator inserted into the 3′ LTR is necessary for a fine-tuned, controlled expression in primary T cells

In LOPIs2-eGFP, a 1.2-kb element (Is2) is inserted into the 3′ long terminal repeat (LTR), probably affecting reverse transcription.[38,39] We therefore generated a panel of LOP constructs harboring different insulator elements inserted at the 3′ of the LVs but outside of the LTR (Figure 2A) and proceed to their analysis as described in Figure S1C. All these elements have been previously described to act as boundaries to enhance transgene expression (Is2, pSAR2, pSAR1, INFβSAR, INFβIgKSAR)[36] and/or insulate (Is2,[36] HS4_650,[40] HS4_Ext[41]) expression cassettes from the effect of surrounding promoters/enhancers. We first investigated the new LOP-eGFP-based LVs in
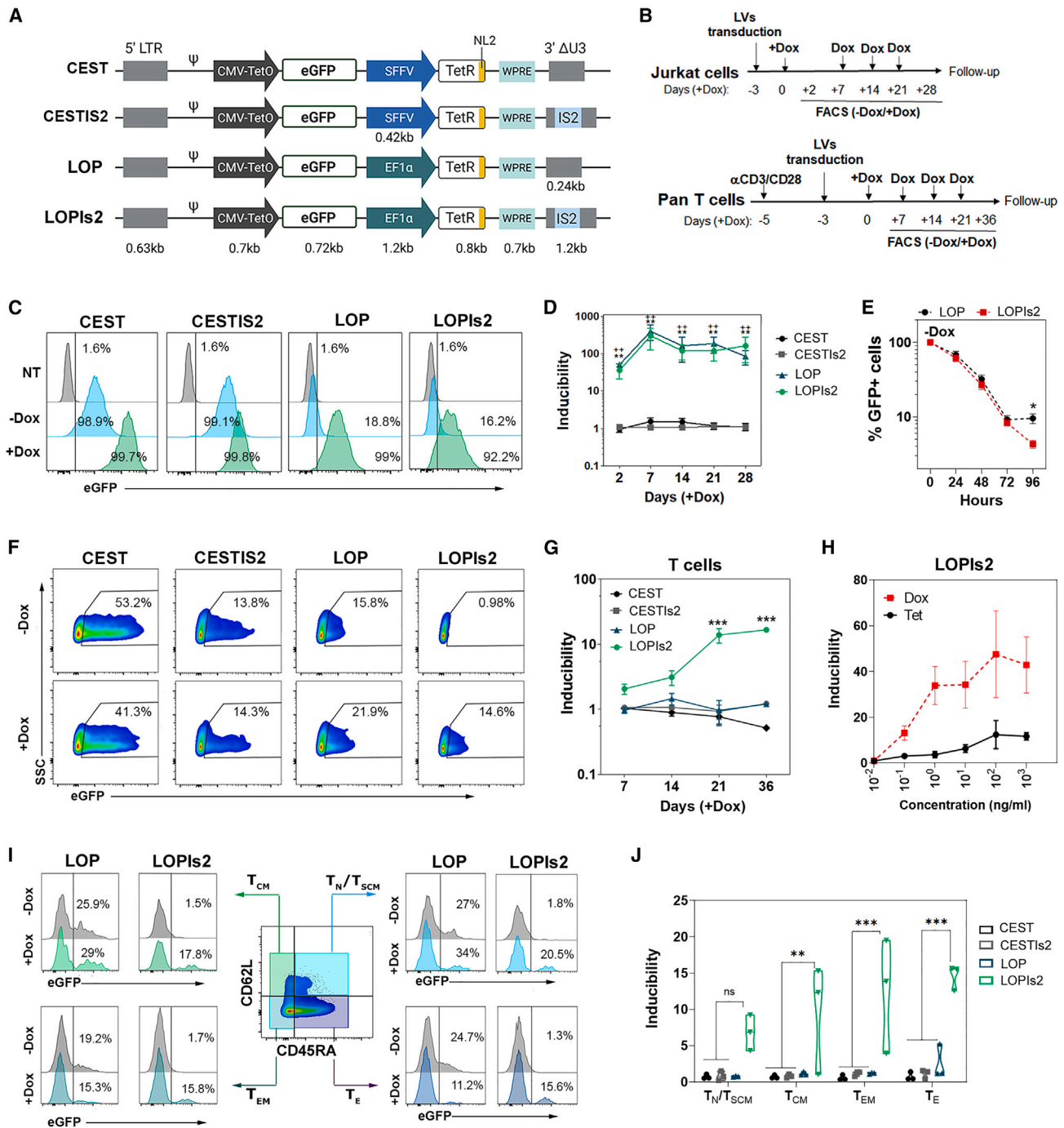
Figure 1. Comparative study of Dox-inducible LVs on Jurkat cell line and primary T cells

(A) Diagram of the different LVs CEST, CESTIs2, LOP-eGFP (LOP) and LOPIs2-eGFP (LOPIs2). Tet repressor (TetR) expression is controlled under the spleen focus forming virus (SFFV) promoter in CEST and CESTIs2 LVs and under elongation factor 1 alpha (EF1α) promoter in LOP and LOPIs2. Insulator Is2 is included in 3′ΔU3. CMV-TetO is the cytomegalovirus promoter with the TetO sequences. Lent-On-Plus vectors include LOP-eGFP (LOP) and LOPIs2-eGFP (LOPIs2) LVs. (B) Experimental timeline of transduction of Jurkat cells (top) and primary T cells (bottom). (C) Representative histograms of sorted Jurkat cells transduced with CEST (1.75± 0.78 vcn), CESTIs2 (0.92 ± 0.03 vcn), LOP-eGFP (LOP) (4.14 ± 1.47 vcn), and LOPIs2-eGFP (LOPIs2) (1.5 ± 0.265 vcn) after 7 days in the presence of 100 ng/mL of Dox. Non-transduced (NT) cells were used as control of negative expression. (D) Inducibility in transduced Jurkat cells up to 28 days. Kruskal-Wallis test, p = 0.01, Bonferroni post-test, two tails. CEST (n = 3),

(legend continued on next page)

immortalized Jurkat T cells and found a clear improvement in viral titer of all constructs (Figure 2B), a tighter control of expression, and/or enhanced transgene expression in the presence of Dox of LTR-out (CEET-Is2, -HS4-650, -Core-ext, and -IFNβSAR) LVs (Figure 2C, top histograms, green and blue lines respectively, and Figure 2E, left graph) compared with LTR-in, LOPIs2 LVs (Figure 2C, top-left histogram). However, these improvements were not maintained in immortalized B cells, Nalm6 (Figure 2C, bottom histograms, and Figure 2E, middle graph) and Namalwa (Figures S1C and 2E, right graph), where the new LOP systems showed no differences.

We next evaluated the new LV systems on primary T cells. In contrast with Jurkat cells, the original LOPIs2-eGFP configuration (with the Is2 inside the 3′ LTR) provided the best regulation and lower leaking in the absence of Dox (Figure 2D, left plots, Figure 2F, and Table 2). Altogether, these results manifest the need for the LOP-eGFP system to be flanked by two Is2 insulators once integrated in the target cells in order to achieve tight control of expression in the absence of the inductor. The effect of the Is2 element on inducibility varies depending on the cell type, with a greater impact in primary T cells. Additionally, this effect is independent of the formula used to determine the inducibility of the different LVs (Table S1). Finally, in order to increase the percentage of LOPIs2-transduced T cells, we optimized the transduction protocol by using different concentrations of Prostransduzin (PTD) and spinoculation (see material and methods for details). Using this protocol, up to 67% of Dox-responsive primary human T cells can be obtained (Figure 2G), which is well in the range of the efficiency required for clinical translation.

LOPIs2 LVs achieved tight regulation of different transgenes in different cell types to generate inducible cell lines

Since the behavior of LVs differs substantially depending on the transgene and on the target cell type, we further investigated the behavior of LOP vectors with Is2 in the LTR (LOPIs2, LOPIs2-eGFP), the only system that did not show leaking in primary T cells. To do this, we first generated new versions of the LOP vectors, called LOP-eN and LOPIs2-eN (Figure 3A) expressing eGFP and Nluc. These LVs allow detection of the expressed transgenes by flow cytometry and bioluminescence for in vitro and in vivo analysis. Next, we evaluated the behavior of these new LVs in different cell types. As observed previously for eGFP transgene, the presence of the Is2 insulator (LOPIs2) improved inducibility (Figure 3B) and reduced leaking (Figure S2B, top) in all the analyzed cell lines (K562, Namalwa, Nalm6, MiaPaCa2, 293T cells), apart from Jurkat cells, where no difference was observed (Figures 1D, 3B, S2A, and

S2B and Table 1). We also corroborated the high sensitivity of the LOPIs2-eN to Dox (0.1–1 ng/mL) in different cell models (Figure S2C) and a complete reversion after 96 h of Dox removal (Figure S2D).

We next investigated the LOPIs2 versatility by expressing different GOIs for applications in gene therapy and/or basic research. We generated two additional LOPIs2 LVs expressing the immature pri-let-7a-3 microRNA (LOPIs2-Let7, Figure 3A) and a third generation αCD19 CAR-2A-tEGFR (LOPIs2-αCD19CAR2AEGFR, hereinafter LOPIs2-CAR) (Figure 3A).

The LOPIs2-Let7 LVs were used to generate cell lines controlling the expression of HMGA2 using Dox (Figure 3C-top). HMGA2 is an essential component of the enhanceosome, which is frequently associated with different types of cancer. For its validation, SK-MES-1 cells (a lung carcinoma cell line) were transduced with LOPIs2-Let7, and three clones were selected and characterized. We observed strong inducibility of the pri-let-7a-3 microRNA (Figure 3C, left graph) with just 10 ng/mL of Dox. As expected, Dox-dependent increase of pri-let-7a-3 microRNA lead to a reduction in HMGA2 mRNA (Figure 3C, right graph).

In the case of LOPIs2-CAR LVs, our purpose was to investigate the ability of the LOPIs2 to regulate a large transgene. As can be observed in Figure 3D, despite the large size of the CAR-2A-tEGFR transgene, a single transduction with LOPIs2-CAR LVs can efficiently generate K562 and Jurkat cells that express the anti-CD19 CAR in their surface only in the presence of Dox.

LOPIs2 LVs can generate functional, transactivator-free, inducible αCD19 CAR-T cells

A main hurdle in gene therapy is to regulate transgene expression (CARs, cytokines, or other GOIs) on cells that are relevant for gene therapy strategies, without affecting their phenotype and function. In order to demonstrate the potency of the LOP system to generate inducible ATMPs, we created the LOP-CAR and LOPIs2-CAR LVs expressing a third-generation αCD19 and tEGFR (Figure 4A, top). Primary T cells transduced with the LOPIs2-CAR LVs generated T cells expressing tEGFR only in the presence of Dox (iCARIs2 T cells). However, as observed for other transgenes, LOP-CAR LVs cannot be regulated in primary human T cells (Figure 4B, middle plots), showing that the Is2 element was indispensable to achieve tight regulation of the CAR on T cells (Figures 4B and 4C). Importantly, the addition of Dox did not alter the normal phenotype of iCARIs2

Table 1. Summary of the behavior (inducibility, leaking, and expression levels) of LOP, LOPIs2, CEST, and CESTIs2 LVs on primary human T cells and Jurkat cells

Cell type	Vector	Transgene	Inducibility	Leaking	Expression levels
T cells	LOP	GFP/CAR	L	H	M
	LOPIS2	GFP/CAR	H	L	M
	CEST	GFP	VL	H	H
	CESTIS2	GFP	VL	H	H
Jurkat	LOP	GFP/GFP-Nluc	H	L	M-H
	LOPIS2	GFP/GFP-Nluc	H	L	M
	CEST	GFP	VL	H	H
	CESTIS2	GFP	VL	H	H
Namalwa	LOP	GFP-Nluc	H	M	M
	LOPIS2	GFP-Nluc	M	L	M
Nalm6	LOP	GFP-Nluc	H	M	M
	LOPIS2	GFP-Nluc	M	L	M
K562	LOP	GFP-Nluc	H	M	M
	LOPIS2	GFP-Nluc	M	L	M
293T	LOP	GFP-Nluc	H	M	H
	LOPIS2	GFP-Nluc	M	L	H
MiaPaCa2	LOP	GFP-Nluc	H	M	M
	LOPIS2	GFP-Nluc	M	L	M

Behavior of LOP and LOPIs2 on Namalwa, Nalm6, K562, 293T, and MiPaCa2 is also indicated. We further analyzed the different cell types in terms of inducibility, leaking, and expression levels. VH = very high; H = High; M = moderate; M-H = moderate–high; L = low; VL = very low.

T cells, as can be observed by the similar percentages of T_{SCM} and T_{CM} subsets in the absence or presence of Dox (Figures 4D and 4E). Also, both T cells subsets are maintained in the CAR– and CAR+ populations in the presence of Dox (Figure 4D, right-bottom plots, and Figure 4E, right bars). Since CAR+ cells will also express the TetR, these data indicate the absence of toxicity of this repressor at the concentrations required to regulate expression on T cells (Figure S3). In addition, we also found that Dox-treated iCARIs2 T cells exhibited a slightly increment in the effector population (Figure 4E, right bars), probably associated with the expression of the CAR, since this effect was not observed in T cells transduced with LOP or o LOPIs2 expressing eGFP (Figure S3).

We next analyzed whether the antitumor activity of iCARIs2 T cells can be controlled by the addition of Dox. Non-transduced T cells (NT) and αCD19 iCAR-T cells were incubated with CD19+ tumor cells (Nalm6 and Namalwa cells) or CD19– cells (K562 cells) (Figure 4F) in the absence or presence of Dox. Our data showed that the killing activity of the iCARIs2-T cells can be controlled by the addition of the inductor (Figure 4G, right plot, and Figure 4H, right and middle graphs) without affecting their activity on CD19– cells (Figure 4H, right graph).

LOP system provided high sensitivity *in vivo*
We next investigated whether the inducible cells generated by transduction of LOP and LOPIs2 LVs can regulate transgene expression

in vivo. For that, we first generated four different cell lines expressing either eGFP (Jurkat-LOP and Jurkat-LOPIs2) or eGFP-Nanoluc (Namalwa-LOP-eN and Namalwa-LOPIs2-eN) using LOP, LOPIs2, LOP-eN, and LOPIs2-eN LVs (Figures 1A and 3A).

Jurkat-LOP and Jurkat-LOPIs2 were inoculated intravenously in NSG mice, fed with jelly containing 0, 200, and 1,000 μg/mL of Dox and sacrificed 3 weeks later (Figure 5A). Engrafted Jurkat cells and eGFP expression levels were analyzed in bone marrow (BM) by flow cytometry (Figure 5B). We hardly detected eGFP expression in mice inoculated with Jurkat-LOPIs2 in the absence of Dox (Figure 5B, right histogram, green line, and Figure 5C). However, eGFP expression was clearly detected in mice inoculated with Jurkat-LOP (Figure 5B, left histogram, green line, and Figure 5C). These data indicate that, although LOP and LOPIs2 LVs behave similarly in Jurkat *in vitro*, the presence of the Is2 element is required to maintain regulation *in vivo*.

A similar experiment was performed with Namalwa-LOP-eN and Namalwa-LOPIs2-eN cells but using lower Dox concentrations (0, 1, and 10 μg/mL) and including a Dox withdrawal of 4 days to measure *in vivo* reversion (Figure 5D). Transgene expression was analyzed at day 12 after Dox administration by bioluminescence in an IVIS analyzer (Figure 5E). Interestingly, both LOP-eN and LOPIs2-eN showed high inducibility and low leaking *in vivo* with just 1 μg/ml of Dox (Figure 5E, left versus middle and right images).
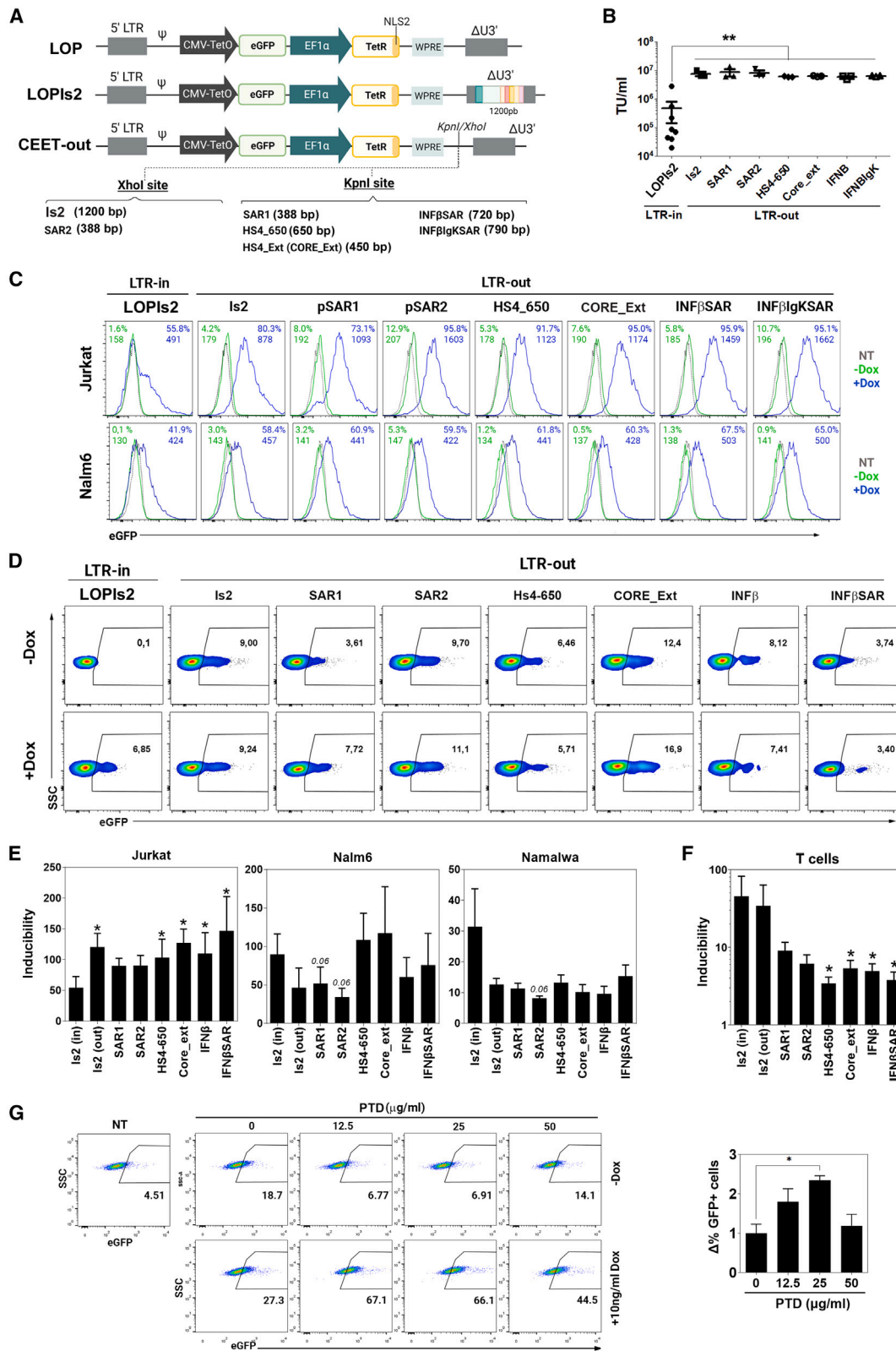
At the endpoint (4 days without Dox), the mice required to be sacrificed due disease progression, and we could only measure eGFP expression in Namalwa-LOP-eN and Namalwa-LOPIs2-eN cells (hCD19+) infiltrated in the BM. These data showed that high Dox concentrations (10 μg/ml) preclude eGFP reversion in both cell lines (Namalwa-LOP-eN and Namalwa-LOPIs2-eN), probably due to longer times for Dox elimination in mice (Figure 5F, purple histograms, and Figure 5G). Although not complete, the reversion in Namalwa-LOPIs2-eN cells was clearly stronger compared with Namalwa-LOP-eN cells (Figure 5F, purple histograms in LOP-eN, versus LOPIs2-eN, and Figure 5G, black squares versus red squares). Importantly, at lower Dox concentrations (1 μg/mL), Namalwa-LOPIs2-eN achieved near-background eGFP expression levels (Figure 5F, right, light-blue histograms, and Figure 5G, red squares, 1 μg/ml) very similar to that found in mice without Dox (Figure 5F, right, green histograms, and Figure 5G, red squares, 0 μg/mL). On the contrary, Namalwa-LOP-eN cells still expressed eGFP even at 1 μg/mL of Dox (Figure 5F, left, light-blue histograms, and Figure 5G, black squares, 1 μg/mL). We next performed a new experiment using even lower Dox concentrations (0, 0.01, 0.1, and 1 μg/ml) in Namalwa-LOPIs2-eN cells. Nanoluc signal could be detected at 0.01 1 μg/ml, showing the high sensitivity of the system (Figure 5H).

Finally, we analyzed the *in vivo* behavior of the LOPIs2 system in primary T cells. We designed an experiment to measure the inducibility and reversion of two different transgenes in the same mice cohort: eGFP expressed by LOPIs2 and CAR expressed by LOPIs2-CAR (Figure 6A). Primary human T cells were independently transduced with LOPIs2 (LOP T cells) and LOPIs2-CAR (iCAR-T cells) LVs and expanded in the absence of Dox. At day 6, LOP T cells and iCAR-T cells were inoculated into Namalwa-NSG mice and fed with gelatin (0.5 μg/ml Dox) (Figure 6A). 4 days after T cell inoculation (also 4 days after Dox administration), we analyzed blood from the different mice and showed expression of CAR (through tEGFR staining) in human T cells. These data evidence the ability of the LOPIs2 LV to regulate expression of the CAR in T cells *in vivo* (Figure 6B). At day 13 (11 days after Dox administration), Dox was withdrawn in two mice in order to evaluate reversion in primary human T cells. At day 20, mice were sacrificed, and eGFP (Figures 6C–6E) and CAR (Figures 6F–6H) expressions were analyzed. eGFP expression was clearly detected in T cells infiltrated in all organs analyzed (Figures 6C–6E, +Dox) and reverted to near-background levels in

the mice in which Dox was withdrawn 7 days earlier (Figures 6C–6E, R). Additionally, antitumoral activity of iCAR-T cells could also be modulated by Dox as shown in Figure 6F. Indeed, the mice treated with the inductor for 20 days (Figure 6F, red circles) had lower tumor burden compared with mice without Dox (Figure 6F, blue circles) or those treated with Dox for 13 days followed by 7 days without Dox (Figure 6F, green circles). This enhanced antitumor activity correlates with higher CAR expression in the presence of Dox (Figure 6G, blue histograms) that reverted when Dox administration is discontinued (Figure 6G, pink histograms, and Figure 6H).

Altogether, these data highlight the applicability of the LOPIs2 platform for *in vivo* applications, working even in a solid-tumor-derived context (Figure S4).

DISCUSSION

Most gene therapies will benefit from spatial and/or temporal control of therapeutic transgenes. Depending on the target disease and the therapeutic strategy, different groups have developed tools for tissue/cell-specific expression,[42–44] physiological/activation-specific expression,[45–48] or externally controlled systems.[6] Here we focus on the development of tools for the generation of smart ATMPs that can be turned on and off by the clinicians by administering ultralow doses of Dox. Several approaches using Veledimex (ecdysone-derivate), mifepristone, or Dox as inductors have been generated (reviewed in Tristán-Manzano et al.[6]). So far, ecdysone-regulated systems (based on the RheoSwitch Therapeutic System [RTS]) are the most successful in therapeutic applications (reviewed in Tristán-Manzano et al.[6]) reaching clinical trials for the treatment of cancer (NCT00815607, NCT01397708, NCT01703754, NCT02423902, NCT02026271, NCT04006119, NCT03679754, NCT03330197, NCT03636477) and localized scleroderma (NCT03740724). However, the GeneSwitch (induced with mifepristone)[17] and Tet-On platforms, probably the most commonly used for basic and applied research, have failed to be translated into clinical settings.[6,49]

A main limitation of all these systems is the requirement of chimeric transcription factors (transactivator); the RTS system requires two chimeric transcription factors (VP16-RXR and Gal4-EcR), the GeneSwitch requires the GLp65 transactivator, and the Tet-On system requires the rtTA transactivator. The constitutive expression of these chimeric proteins induces different types of alterations on the

---

Figure 2. Behavior of LOP-derived LVs harboring different insulators in cell lines and primary human T cells

A) Diagram of LOP-eGFP (LOP) lentiviral vector with Is2 insulator inside the LTR (LOPIs2-eGFP, LTR-in) or Is2, pSAR1, pSAR2, HS4_650, Core_ext, IFNβ, and IFNβSAR insulators outside the LTR (LTR-out) in KpnI/XhoI sites (see material and methods). (B) Effective viral titer (TU/ml) calculated in Jurkat cells. Kruskal-Wallis test, p < 0.001 one-way ANOVA T test, significant = p < 0.05. (C) Representative histograms of eGFP expression driven by the different LVs in Jurkat (top) and Nalm6 (bottom) cells in the absence (green) or presence (blue) of Dox (10 ng/mL) at day 12 post-transduction. NT, dotted gray line. The percentage of eGFP+ cells and the MeFI of the total population in –Dox and +Dox conditions are indicated in green (top-left of each histogram) and blue (top-right of each histogram) respectively. (D) Representative dot-plot of eGFP expression driven by the different LVs in primary T cells in the absence or presence of Dox (10 ng/mL) at day 21 post-transduction. The percentages of GFP+ cells are indicated. (E) Graphical representation of the inducibility of each LV in Jurkat (left, n = 4), Nalm6 (middle, n = 3) and Namalwa (right, n = 3). Wilcoxon test, one-tailed. (F) Graphical representation of inducibility of each LV in primary T cells (n = 4). Wilcoxon test, one-tailed. (G) Left, representative dot-plots of primary T cells transduced with LOPIs2-eGFP in the presence of different concentrations of Protransduzin (PTD). eGFP expression was determined 10 days post-TD and 7 days post-Dox addition (10 ng/ml). Percentages of GFP+ cells are indicated. Right, graph showing increment in the percentage of eGFP+ cells with different amounts of PTD. Wilcoxon test, two-tailed (n = 3).

Table 2. Summary of inducibility (I), leaking (L), and expression levels (E.L.) of LOPIs2 LVs (top) and the new LVs harboring different elements outside the LTR (bottom) in T cells, Jurkat, Namalwa, and Nalm6

Cell type		T Cells			Jurkat			Namalwa/Nalm6		
Behavior		I	L	E.L.	I	L	E.L.	I	L	E.L.
LTR-In	LOPIs2	H	L	M-H	H	L	M	H	L	M
	LOP-Is2out	H	H	M-H	VH	L	H	M	M	M
	LOP-SAR1	M	H	M-H	H	L	H	M	M	M
	LOP-SAR2	M	H	M-H	H	L	H	M	M	M
LTR-out	LOP-HS4-650	M	H	M-H	VH	L	H	H	M	M
	LOP-CORE_Ext	M	H	M-H	VH	L	H	H	L	M
	LOP-INFbeta	M	H	M-H	H	L	H	H	L	M-H
	LOP-INFbetaIgKSAR	M	H	M-H	VH	L	H	H	L	M-H

In gray is indicated the best LVs for each cell type. VH = very high; H = high; M = moderate; M-H = moderate-high; L = low.

target cells due to their ability to sequester transcription factors and to activate cellular genes (reviewed in Tristán-Manzano et al.[6]). In this manuscript, we have designed different all-in-one, transactivator-free LVs that differ in their inducibility and leakiness depending on the cell type and have shown their ability to generate first-in-class, Dox-inducible, transactivator-free ATMPs. This platform provides a precise, fine-tuned regulation, is versatile and applicable to all cell types analyzed, and allows regulation with ultralow doses of Dox.
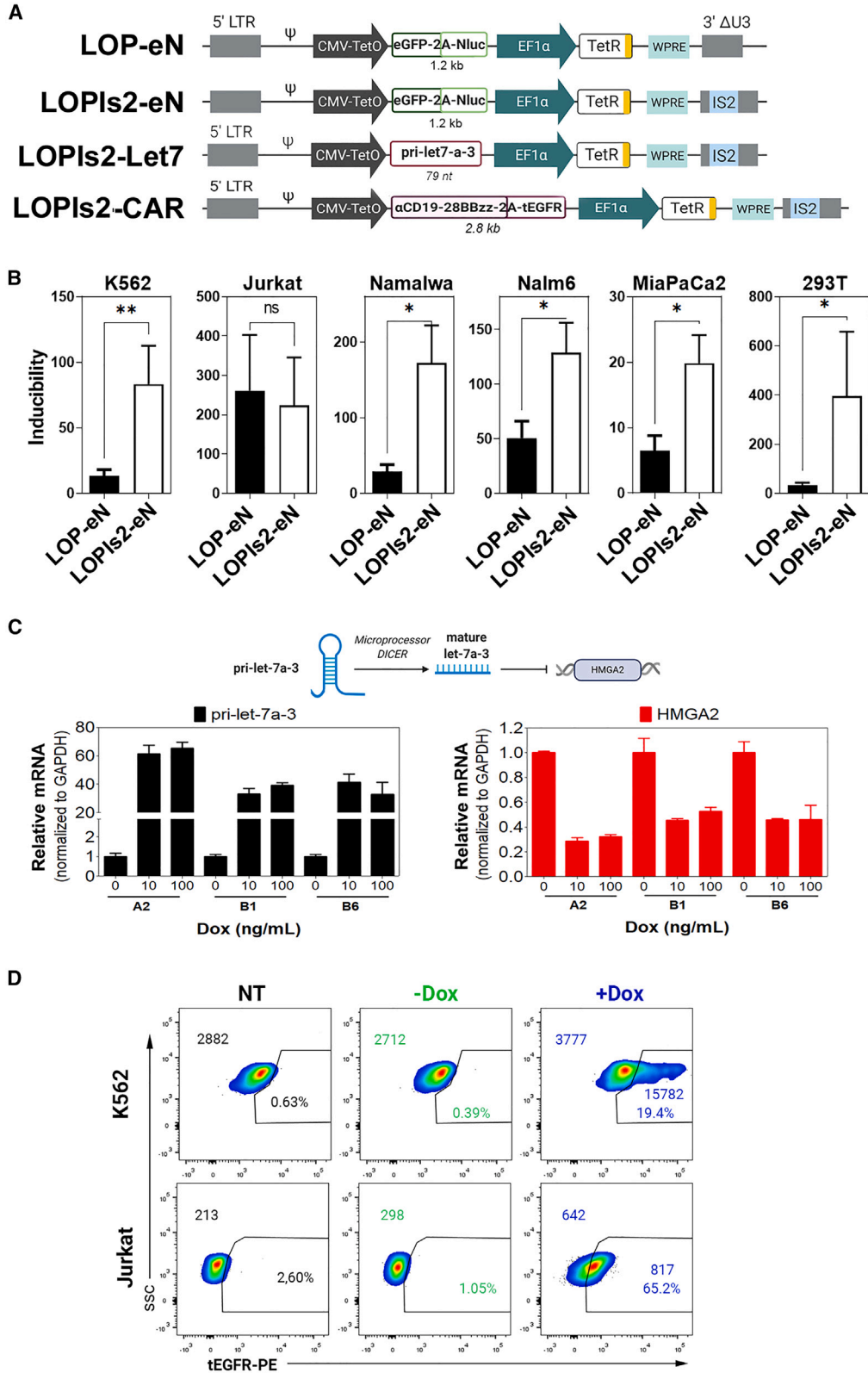
Since T cells are one of the most important targets for the generation of ATMPs, we first studied the ability of LOP and CEST LVs (the only Dox-responsive all-in-one systems free of transactivators)[35] to regulate eGFP in primary human T cells. Both systems are all-in-one LVs that include a TetR expression cassette and a Dox-responsive promoter expressing eGFP but differing in the promoter used to drive TetR expression. The CEST LVs use the spleen focus-forming virus promoter and achieved very high inducibility and expression levels, although leaking is a main problem of this system.[35] On the contrary, the LOP LVs using the long EF1α promoter to drive TetR expression achieved very high inducibility and tight regulation but with moderately low expression levels.[37] We showed previously that this reduction in leaking in LOP LVs is due to a negative interference between the CMV-TetO and the EF1α promoters, which leads to lower expression levels from the CMV-TetO, facilitating its regulation by TetR.[37] In addition to CEST and LOP, we included in the analysis the CESTIs2 and the LOPIs2, incorporating the Is2 insulator inserted into the 3′ LTR. The Is2 element combines a 650-bp fragment of the HS4 insulator together with a synthetic SAR element,[36] and we have shown previously that the insertion of Is2 into the 3′ LTR of LVs improves their expression efficiency and avoids their silencing in embryonic human cells.[36] We showed here that only the LOPIs2 systems regulate transgene expression in all primary human T cells subsets, with minimal leaking and moderate expression. Contrary to what was observed in other cell lines, none of the other inducible LVs analyzed managed to control expression in this cell type. Of note,

several of the new LVs behave better that the LOPIs2 to regulate transgene expression in immortalized cell lines (see Tables 1 and 2).

Importantly for clinical applications, the LOPIs2 LVs generated inducible T cells that responded to ultralow doses of Dox, 10–100 times below the concentrations required to kill bacteria, reducing dramatically the probabilities to generate resistance and interference with the endogenous microbiota of the patient. The requirement of the Is2 insulator in the LOP system to regulate primary T cells was unique of these cells, as LOP LVs managed to regulate (although less efficiently) all other cell types analyzed previously, including immortalized T cells (Jurkat) (this manuscript and Benabdellah et al.[37]). These data highlight the importance of the cellular context in the behavior of LVs. As a downside, the inclusion of the 1.2-kb Is2 element into the LTR reduced viral titer 2–4 times. We therefore generated different LOP (CEET) systems harboring the Is2 and other insulators outside the 3′ LTR that provided different LVs (CEET_Is2out, CEET_HS4-650, CEET_Core-ext, and CEET_IFNβSAR). These modifications improved titer, expression levels, and inducibility when analyzed in several immortalized cell lines. However, all these new CEET-derived LVs lost inducibility on primary T cells due to a clear increment in expression in the absence of Dox.

Once we selected the LOPIs2 as the best LV for the generation of inducible ATMPs, we demonstrated its ability to generate different inducible cell lines expressing different transgenes of different sizes (eGFP-Nanoluc, pri-let7-a-3, αCD19CAR-tEGFR). We took advantage of the LOPIs2-eN LVs (expressing eGFP and NanoLuciferase) to study the responsiveness of the system *in vivo* using two different cell lines. Interestingly, we showed *in vivo* transgene induction at 10 ng/ml, which is 10–100 times lower than that reported by other systems.[21–23] Furthermore, once the cells were recovered from the mice, they maintained a similar inducibility and percentage of expression as before their inoculation, suggestive of the robustness of the expression and the absence of deleterious genotoxic or silencing

A

LOP-eN
5' LTR | Ψ | CMV-TetO | eGFP-2A-Nluc (1.2 kb) | EF1α | TetR | WPRE | 3' ΔU3

LOPIs2-eN
Ψ | CMV-TetO | eGFP-2A-Nluc (1.2 kb) | EF1α | TetR | WPRE | IS2

LOPIs2-Let7
5' LTR | Ψ | CMV-TetO | pri-let7-a-3 (79 nt) | EF1α | TetR | WPRE | IS2

LOPIs2-CAR
5' LTR | Ψ | CMV-TetO | αCD19-28BBzz-2A-tEGFR (2.8 kb) | EF1α | TetR | WPRE | IS2

B

K562 ** / Jurkat ns / Namalwa * / Nalm6 * / MiaPaCa2 * / 293T *

(Inducibility comparing LOP-eN vs LOPIs2-eN)

C

pri-let-7a-3 → Microprocessor DICER → mature let-7a-3 ⊣ HMGA2

pri-let-7a-3: Relative mRNA (normalized to GAPDH)
Dox (ng/mL): A2 (0, 10, 100), B1 (0, 10, 100), B6 (0, 10, 100)

HMGA2: Relative mRNA (normalized to GAPDH)
Dox (ng/mL): A2 (0, 10, 100), B1 (0, 10, 100), B6 (0, 10, 100)

D

	NT	-Dox	+Dox
K562	2882 / 0.63%	2712 / 0.39%	3777 / 15782 / 19.4%
Jurkat	213 / 2,60%	298 / 1.05%	642 / 817 / 65.2%

SSC (vertical axis), tEGFR-PE (horizontal axis)

(legend on next page)

effects of the LOPIs2 system. In addition, 4 days of Dox withdraw *in vivo* were sufficient to almost reach basal levels. Importantly, we have also demonstrated that the LOPIs2 system can regulate (ON/OFF) two different transgenes in primary human T cells, evidencing its potential for the generation of inducible ATMPs.

For gene therapy applications, the aim of inducible systems must be to provide a new function that can be controlled by the addition of a drug. Therefore, to validate LOPIs2 as a tool for the development of smart ATMPs, we generated inducible SK-MES-1 cell lines and inducible CAR-T cells and analyzed whether we could control the desired function. Inducible SK-MES-1 cells were engineered to express the immature pri-let-7a-3 microRNA upon Dox addition and demonstrated their functionality by showing the downregulation of the oncogene HMGA2 (a let-7a-3 microRNA target).

Special interest was put into demonstrating the ability of LOPIs2 to generate fully functional, inducible CAR-T cells. CAR-T therapies are one of the most promising fields in immunotherapy, but their effectiveness against solid tumors is still far away from clinical success. New approaches to provide greater CAR-T cell potency are required, and with this, new ways to control this potency are mandatory. Different strategies to control CAR-T function and potency are currently being investigated.[6,50] First attempts to control CAR-T cells aimed at their destruction in case of serious side effects by using "suicide switches"[51] or the proteolysis degradation of the CAR protein by promoting ubiquitination.[52] However, these systems do not address the *on-target off-tumor* toxicity due to share antigen recognition between tumors and healthy tissues. To tackle this problem, different groups focused on the development of self-regulating systems and complex "logic gating" approaches.[50,53–55] These strategies aim at enhancing the efficacy of CAR-T cells using complex mechanisms that enable targeting their activation only at the tumor sites when two or more signals get together (AND), when either signal is present (OR), or when one is present and the other is not (NOT). The outcome of the final signal is to induce the expression of additional CARs or/and molecules that enhance antitumor efficacy. The different logic gating systems can allow the autoregulation of the CAR-T cells to modulate immune responses on healthy tissues, to secrete potent immunostimulatory molecules only into the tumor sites, and to reduce the likelihood of tumor antigen escape. However, in most of these systems, once the CAR-T cells are inoculated into the patients, the clinician cannot intervene on their potency and/or type of activity.

Since LOPIs2 LVs have limited cargo capacity and low expression levels, the LOPIs2 platform is not intended to replace logic gating strategies. Rather, it is envisioned as an additional tool to enhance the external control of these living drugs. For example, by using Dox-inducible LVs, we could generate logic gating that is only active in the presence of Dox. As proof of concept, we generated CAR-T cells that expressed the CAR only in the presence of Dox and showed that we could externally control their antitumor activity both *in vitro* and *in vivo*. Interestingly, the phenotypes of the LOPIs2-eGFP-transduced T cells and iCAR-T cells were identical to unmodified T or CAR-T cells (respectively), indicating absence of toxicity of the TetR. Importantly, the absence of phenotypic alterations was also observed after the addition of Dox in both inducible T cells, maintaining similar percentages of T_{CM} and T_{SCM} subpopulations after induction. The maintenance of these populations in both Dox-inducible T cells (LOPIs2-eGFP-transduced T cells and iCAR-T cells) indicates that this platform can be used for the generation of inducible ATMPs without substantial alterations in their functionality. These data contrast with the systems using transactivators where different publications have shown several alterations on the inducible cells generated with these systems.[24–27] Particularly relevant is the work of Smith et al.[28] showing a depletion of antigen-experienced T cells in rtTA-transgenic mice. A few groups have used transactivator-based systems for CAR-T applications.[4,9,56–58] Although these systems have shown good regulation (some of them with higher leaking than others), all require higher doses of Dox 100 ng/ml to 4 μg/mL that can be a limitation for multiple applications (reviewed in Tristán-Manzano et al.[6]). More importantly, none of these works characterize T cell phenotype due to transactivator expression, which may trigger critical effects as discussed here. A potential downside of the LOP system is the lower kinetics to achieve reversion. Indeed, contrary to rtTA-based systems, once doxycycline has been removed, the TetR need to accumulate at enough concentration to block again the transcription process, making repression a slow process. As mentioned before, important constraints of the LOP system are its restricted cargo capacity and low expression levels. The latter is likely the primary reason for the iCAR's reduced efficiency compared with constitutive CARs. To overcome this, we suggest utilizing the LOP platform for generating iTRUCKs that express CARs via a constitutive or physiological (Tristán-Manzano et al.[59]) promoter and cytokines (or other highly bioactive proteins) via the LOP system.

The potential immunogenicity of TetR in the context of T cells is a common problem for both TetR- and TetR-transactivator-based systems. The immunogenicity of the latter has been studied in detail,

Figure 3. LOPIs2 LV is a versatile tool to generate transactivator-free inducible cell lines expressing different transgenes

A) Diagram of the different LOP LVs used: LOP-eN and LOPIs2-eN LVs express eGFP-P2A-Nanoluc, LOPIs2-Let7 express pri-let-7a microRNA, and LOPIs2-CAR express αCD19-CAR-41BB-CD28-T2A-tEGFR. (B) Graphs showing inducibility of LOP-eN and LOPIs2-eN LVs in different cell lines. Non-parametric Mann-Whitney test, two tails, at least n = 3 for each cell type. (C) Top: representation of prit-Let7-a-3 microRNA processing and inhibition of its target HMGA2. Left graph: relative prit-Let7-a-3 mRNA levels (normalized to GAPDH) of three different clones (A2, B1, B6) of LOPIs2-Let7 transduced SK-MES cell line in the absence or presence of 10 and 100 ng/mL of Dox. Right graph: relative HMGA2 mRNA levels (normalized to GAPDH) of three different clones (A2, B1, B6) of transduced SK-MES cell line in the absence or presence of 10 and 100 ng/mL of Dox. (D) Dot-plots of transduced K562 and Jurkat cells with LOPIs2-CAR LVs in the absence or presence of 10 ng/ml of Dox, determined by tEGFR expression. Percentage of CAR+ cells and MeFI of total population (outside the gate) and of CAR+ cells (for +Dox, inside the gate) are indicated in the figure.
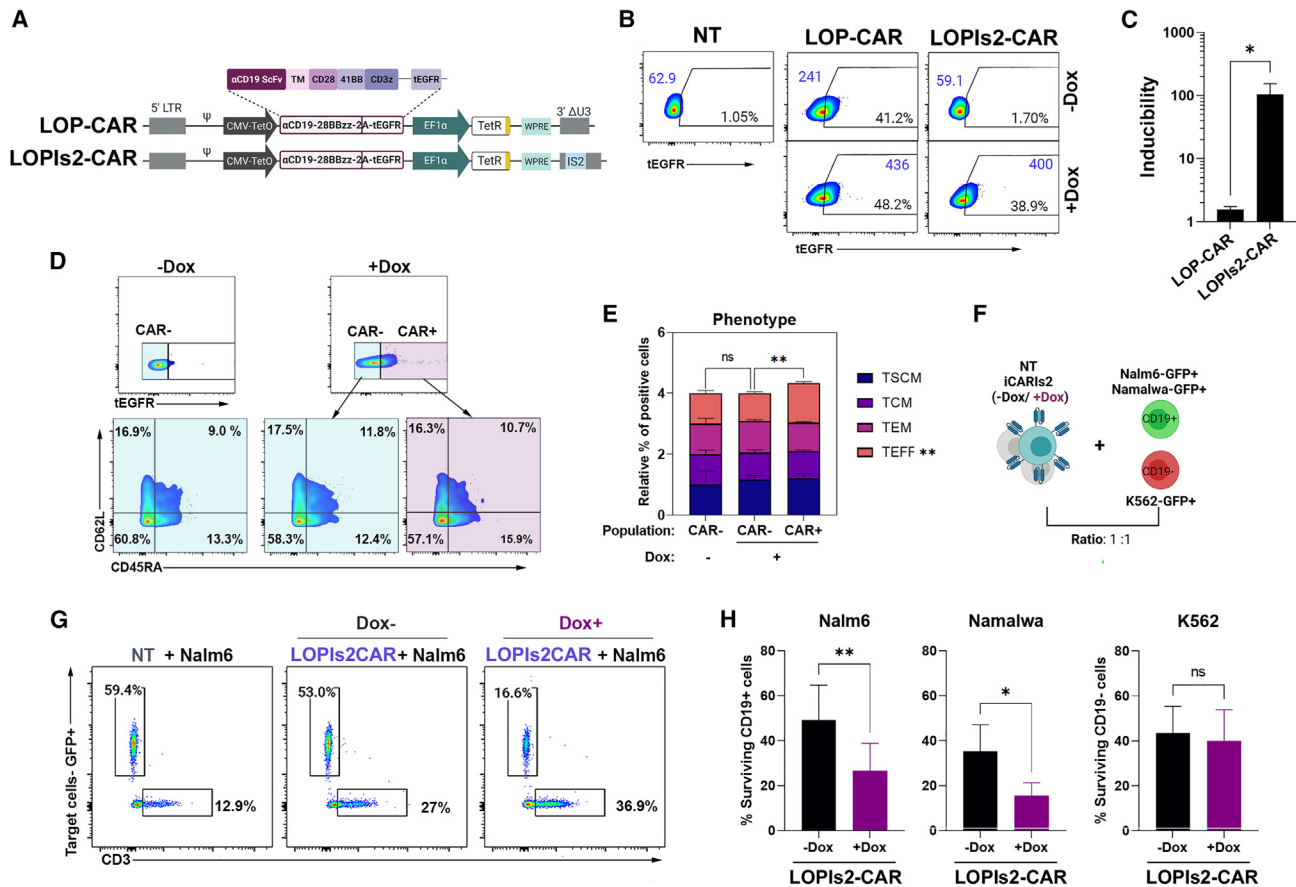
Figure 4. LOPIs2-CAR LVs generate first-in-class, transactivator-free, inducible CAR-T cells without altering T cell phenotype

(A) Schematic representation of LOP-CAR and LOP-CARIs2 LVs encoding for a third-generation αCD19-CD28-41BB-CD3z with a T2A sequence and the truncated EGFR as selection marker. (B) Representative dot-plots of LOP-CAR and LOPIs2-CAR expression in primary T cells in –Dox and +Dox (10 ng/ml) conditions at 10 days post-transduction. Non-transduced cells (NT) are used to establish CAR (tEGFR) background. MeFI values of total population (left) or those of the CAR+ cells (right) are indicated in blue color. (C) Inducibility of LOP-CAR and LOPIs2-CAR expression in transduced T cells. Mann-Whitney test, two tails. *p < 0.05 (n = 4). (D) Representative dot-plots of CD45RA/CD62L expression analyzed in CAR– and CAR+ gate in the LOPIs2-CAR in presence or absence of Dox. Percentage of positive populations are indicated. (E) Percentage of positive cells of T_{SCM}, T_{CM}, T_{EM}, and T_{EFF} in the selected gates. Non-significant Kruskal-Wallis test, Mann-Whitney *p < 0.05 of T_{EFF} subset of CAR– (Dox+) vs. CAR+ (Dox+). (n = 4). (F) Scheme of the cytotoxic assay based on the co-culture of a bulk population of LOPIs2-CAR and target (CD19+) and control (CD19–) cells for 48 h. iCARIs2 T cells were 15%–20% of CAR+. (G) Representative dot-plots of NT, LOPIs2-CAR (–Dox), and LOPIs2-CAR (+Dox) T cells co-cultured with Nalm6-eGFP-Nluc+ target cells during 48 h. iCARIs2 T cells kill CD19+ cells only in the presence of Dox (right plot). Percentage of positive cells are indicated in the figure. (H) Graph showing the percentage of CD19+ cells (Nalm6 and Namalwa) and CD19– cells (K562) in the absence or presence of Dox after incubation with iCARIs2 T cells. *p < 0.05 (n = 4). Paired T test, two tails. Wilcoxon test, two-tailed.

showing both cellular and humoral responses leading to a lack of regulation.[60,61] Although immunogenicity of the TetR-based systems is poorly characterized, its bacterial origin anticipates immune responses that can compromise future gene therapy applications. In this line, a further characterization of TetR levels and possible immunogenicity with our lentiviral systems compared with TetR-VP16 transactivator systems will be performed prior to application in clinical trials. Probably, final strategies using TetR-based systems should include additional strategies to ameliorate or avoid immune responses. Antigen-specific tolerance strategies[62] or more specific TetR designs could be used. For instance, the glycine-alanine repeat of Epstein-Barr virus antigen 1 has been involved in immune evasion

by blocking proteosomal degradation[63] and has been used recently to evade host immune responses against rtTA protein.[64] A similar approach could be used to improve the *in vivo* behavior of TetR-based systems.

The inducer and its characteristics constitute another key parameter for the benefits of the therapy. Dox is an antibiotic derived from tetracyclines, with a small size and polar character that allows it to be permeable to the blood-brain barrier. The inducible cell lines generated with the LOPIs2 responded to ultralow doses of Dox both *in vitro* (0.1 ng/mL) and *in vivo* (10 ng/mL), being between 10 and 100 times more sensitive than the systems described so far.[6]
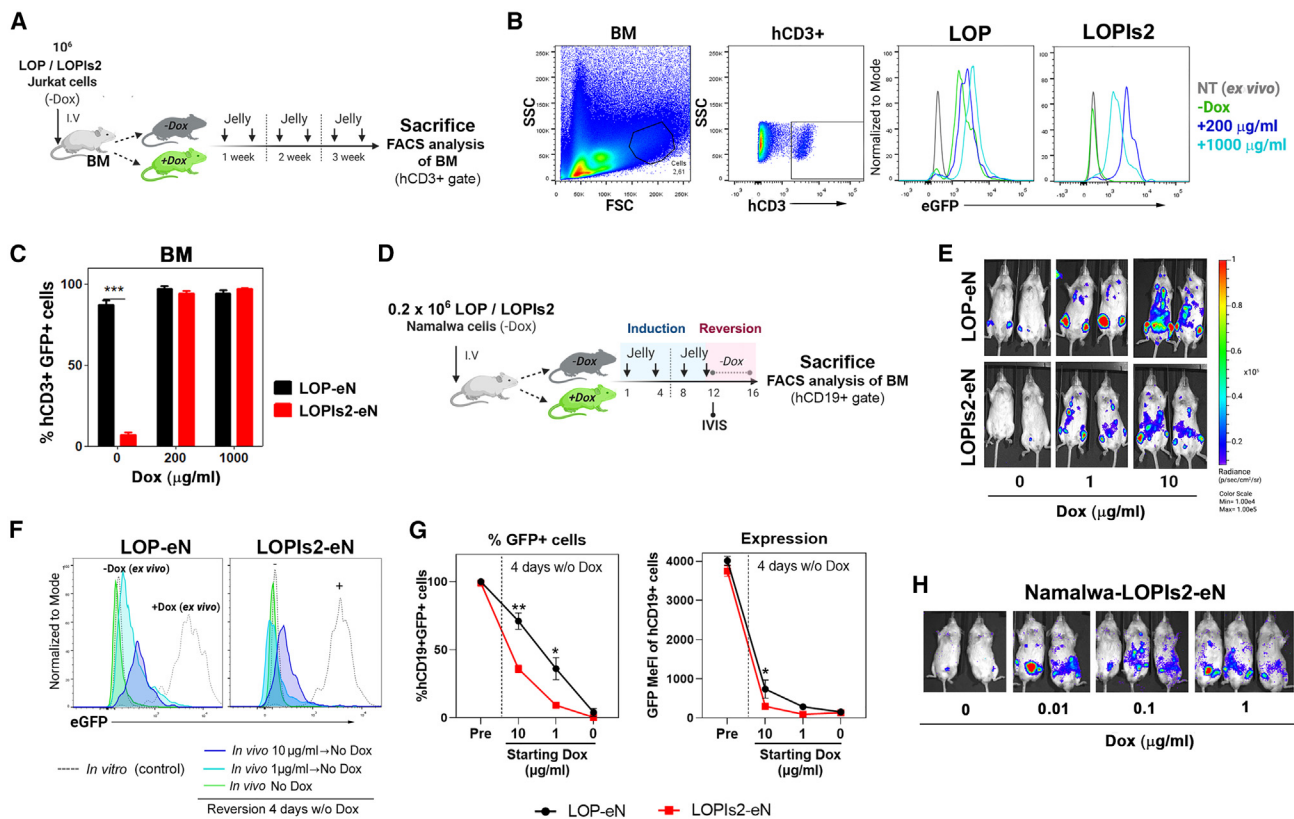
Figure 5. *In vivo* evaluation of Lent-On-Plus LVs behavior in cellular models

(A) Schematic generation of the Jurkat model and timeline of the experiment. (B) Left plots: gating strategy to analyze human CD3+ cells (Jurkat) engrafted in the bone marrow of transplanted mice. Right histograms showing a representative experiment to detect eGFP expression driven by LOP- or LOPls2-Jurkat cells after engraftment in the bone marrow of mice supplemented with no Dox (green), 200 µg/mL (dark blue), and 1,000 µg/mL (light blue) compared with NT (*ex vivo*, gray) background. (C) Percentage hCD3+ eGFP+ Jurkat cells transduced with LOP (black bars) and LOPls2 (red bars) LVs in bone marrow of mice supplemented with 0, 200, or 1,000 µg/mL of Dox. N = 2 for each group. Bonferroni multiple comparison test, ***p < 0.001. (D) Scheme to generate LOP-eN- and LOPls2-eN-Namalwa mice models and timeline of the experiment for IVIS (E) and reversion (F) analysis. (E) Bioluminescence images (IVIS) of mice inoculated with LOP-eN- and LOPls2-eN-transduced Namalwa cells at day 12 post inoculation and supplemented with 0, 1, or 10 µg/mL. (F) Representative histograms showing eGFP expression by FACs in LOP-eN- (left) and LOPls2-eN-Namalwa (right) cells pre-inoculation in the presence or absence of Dox (empty histograms, gray dashed lines, + Dox and –Dox) and isolated from bone marrow of mice previously treated with 10 µg/mL (dark purple), 1 µg/mL (light blue), or no Dox (green) and then kept 4 days without Dox for reversion. (G) Graphs showing percentage of eGFP+ cells (left) and MeFI (right) of hCD19+ cells in LOP-eN- (black squares) and LOPls2-eN- (red squares) cells at pre-inoculation (pre) or after being isolated from the bone marrow of mice previously treated with 10, 1, or 0 µg/mL of Dox and then treated for 4 days without Dox. Bonferroni multiple comparison test. *p < 0.05; **p < 0.01. (H) Bioluminescence of mice inoculated with LOPls2-eN-Namalwa cells and orally supplemented with 1, 0.1, 0.01, or 0 µg/mL of Dox.

The existing Tet-On vectors required doses ranging from 10 ng/ml to 4 g/ml of Dox, overlapping with the doses required as antibiotic and are therefore susceptible to generating antibiotic resistance and other side effects in case of prolonged or intermittent exposure, not to mention to causing collateral damage to self-microbiota, which play a major role in several immune syndromes. Indeed, it has been observed that sub-inhibitory concentrations of bacterial growth (150 ng/mL) are capable of inducing resistance and that it can be favored in stressful environments,[65] such as tumors. Also, exposure to Dox within the classical range in Tet-On system (100 ng–10 µg) has been shown to alter the metabolism and proliferation of certain human cells in a dose-dependent manner.[66] Therefore, only the newest generation of the rtTA systems and the LOP platform would be adequate to avoid these metabolic alterations due to the administration of Dox.

MATERIAL AND METHODS
Cells lines

Jurkat (TIB-152), Namalwa cells (CRL-1432), Nalm6 (CRL-3273), and K562 cells (CCL-243) were purchased from the ATCC and cultured in RPMI-1640 media supplemented with 10% fetal bovine serum (FBS) and 100 U/mL penicillin/streptomycin (1%P/S, Biowest) at 37°C in a 5% CO_2 and 85%–90% humidified incubator. HEK-293T cells were cultured in high-glucose Dulbecco's Modified Eagle's Media (DMEM, Biowest) supplemented with 10% FBS (Invitrogen) at 10% CO_2 atmosphere. MiaPaCa2 (CRL-1420) were cultured in
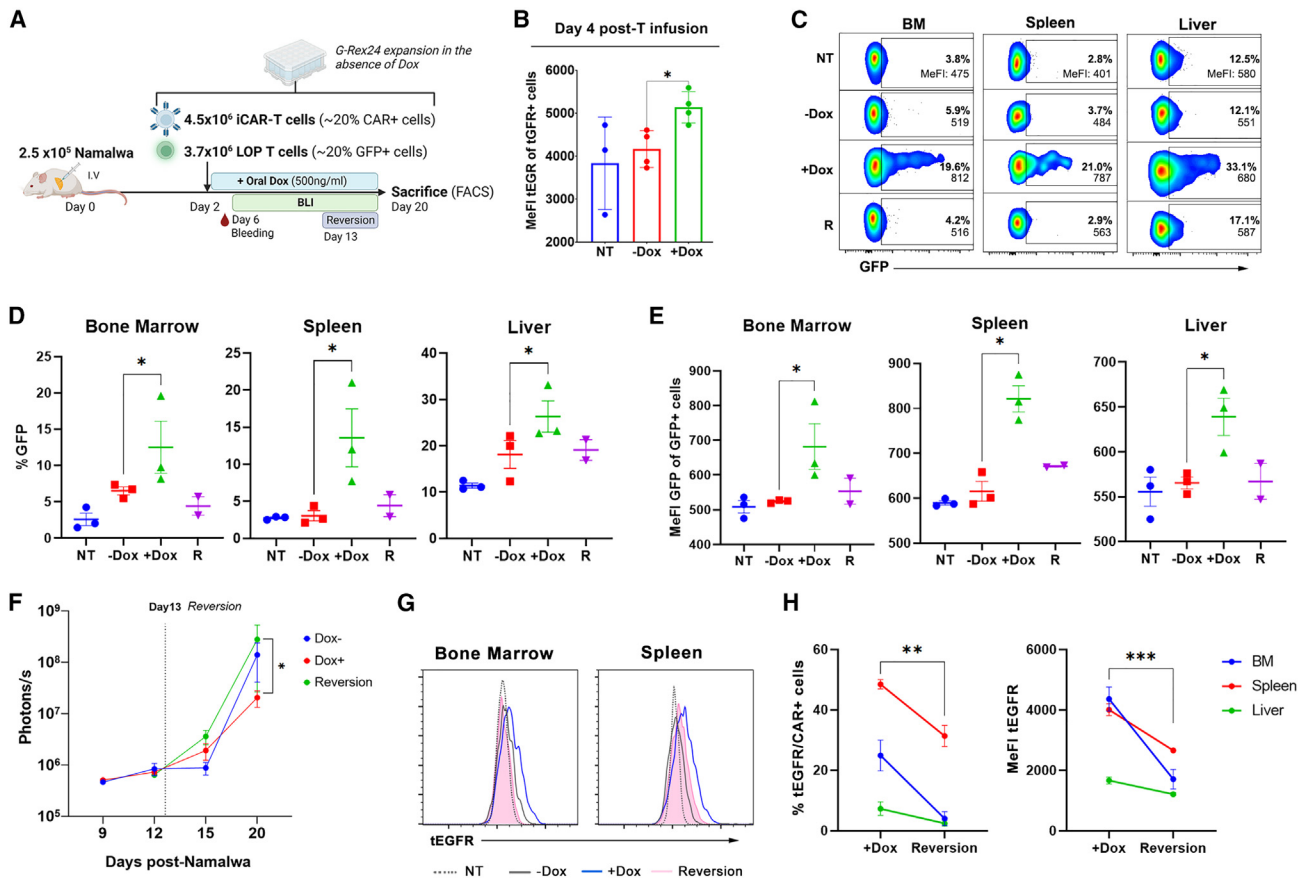
Figure 6. *In vivo* evaluation Lent-On-Plus LV behavior in primary human T cells

A) Schematic generation of the *in vivo* experiment. Primary human T cells were transduced separately with LOPIs2 and LOPIs2-CAR LVs to express GFP and CAR/tEGFR in an inducible manner. Transduced cells were cultured in a G-Rex24 plate for 7 days in the absence of Dox prior to inoculation into NSG mice (previously inoculated with tumoral Namalwa-GFP-NLuc cells). Three mice were inoculated with untransduced T cells (NT). 8 mice were inoculated with iCAR-T cells (4.5×10^6) and LOP-T cells (3.7×10^6) at the same time. These mice were separated in two groups of four to be fed with gelatin without Dox (–Dox) or with 500 ng/ml of Dox (+Dox). (B) Graph showing expression of the CAR determined as tEGFR expression in T cells isolated from the blood of mice inoculated with untransduced T cells (NT) or transduced T cells in the absence (–Dox) or presence (+Dox) of doxycycline at day 4 days post-T cells inoculation. Non-parametric Mann-Whitney test, *p < 0.05. (C) Representative dot-plots of GFP expression from T cells (hCD3+ cells) engrafted in bone marrow (BM), spleen, and liver. Percentage and MeFI of GFP in GFP+ cells is indicated. (D and E) Percentage (D) and expression (E) of GFP in hCD3+ isolated from the different organs. Non-parametric Mann-Whitney test, *p < 0.05. N(NT) = 3; N(–Dox) = 3; N(+Dox) = 3; N(R) = 2. (F) BLI determined as photons/s (indicative of tumor burden) in mice without Dox (blue), with Dox (red), and after reversion from day 13 (green). Two-way ANOVA, Tukey's post test. (G) Representative histograms showing CAR-tEGFR expression in T cells present in bone marrow (left) and spleen (right) from mice inoculated with NTD T cells (dashed and gray line) and mice inoculated with transduced T cells and left without Dox (gray line), with Dox up to day 20 (blue line) or with Dox for 13 days and then left without Dox for 7 days (pink line). (H) Percentage (left) and MeFI (right) of CAR/tEGFR expression from mice treated with Dox for 20 days (+Dox) and mice treated with Dox for 13 days and 7 days without (Reversion) at final point in the indicated organs. Two-way ANOVA, **p < 0.01 and ***p < 0.001.

DMEM supplemented with 10% FBS and 1% P/S, and SK-MES-1 (HTB-58) cells were cultured with DMEM (Gibco) supplemented with GlutaMAX, 10% FBS, and 100 U/mL of P/S (Invitrogen). Cells were maintained in incubators at 37°C with 5% CO_2 atmosphere and 85%–90% relative humidity. Absence of *Mycoplasma spp.* in cultured cells was routinely tested by a PCR-based assay (Minerva).

Primary T cells

Human primary T cells were isolated from fresh or frozen peripheral blood obtained from healthy donors at the Hematology Department of Hospital Universitario Reina Sofía (Córdoba, Spain). All donors gave their written informed consent, and the study was performed according to the guidelines of the Regional Government Junta de Andalucía-Consejería de Salud ethics committee and requirements under the Spanish specific regulation (RD 1301/2006) and International Conference of Good Clinical Practice. Blood was diluted 1/2 to 1/4 in PBS, and mononuclear cells were collected after Ficoll separation (Lymphosep, Biowest). Cells were washed twice at 200 *g* for 10 min, and then, Pan-T cells were isolated following MACS Express Separator (Miltenyi Biotec) protocol and then seeded at 10^6 cells/ml in TexMACS supplemented with interleukin-2 (IL-2) (20 IU/mL, Miltenyi Biotec). T cells were activated with TransAct (Miltenyi

Biotec) during 48 h before lentiviral transduction following the manufacturer's recommendations.

Plasmids

All-in-one systems (CESTnl2 and CESTnl2Is2)[35] and LOP systems (LOP-eGFP [CEET], and LOPIs2-eGFP [CEETIs2])[37] were previously described. Based on LOP-eGFP and LOPIs2-eGFP, we constructed LOP-eN and LOPIs2-eN that express eGFP-P2A-NanoLuc[59] under the CMV-TetO promoter. eGFP-P2A-NanoLuc was flanked by AscI/SbfI restriction sites and synthesized by Genescript (Genescript, NY, USA). Third-generation anti-CD19-CAR (clone FCM63, αCD19-28-BB-zz) that includes the CD28, 4-1BB, and CD3z intracellular domains and truncated EGFR as selection marker was purchased from Creative Biolabs. This insert was cloned into LOP-eN and LOPIs2-eN backbones once subcloned into a modified pUC19 with EcoI/BamHI enzymes to provide AscI/SbfI restriction sites. Pri-let-7a3 was amplified from 150 ng of SK-MES-1 genomic DNA with High Fidelity PCR System (Roche) following the manufacturer's instructions, using primers that added AscI and SbfI restriction sites at the 5′ and the 3′ ends of the amplicon, respectively (AscI_Prilet7a3_Fw and SbfI_Prilet7a3_Rv). Then, pri-let-7a3 was cloned using AscI and SbfI sites in LOPIs2-eN backbone to obtain LOPIs2-pri-let-7a-3. Primers used were as follows: AscI_Prilet7a3_Fw: AAAGGCGCGCCTGCCCGCCAGAATCCCT and SbfI_Prilet7a3_Rv: TTTCCTGCAGGTCACACAGCAAGTGGCACCTAG.

Insulators

Novel insulated vectors are based on LOP-eGFP LV. The Is2 element, which combines the HS4-650 fragment and the SAR2, was designed and synthesized as previously described in Benabdellah et al.[36] CEET-Is2 (out LTR) was generated by inserting the Is2 element into the unique XhoI site of the LOP-eGFP. CEET-SAR 1, CEET-SAR2, CEET-HS4_650, CEET-Core_Ext, CEET-INFβSAR, and CEET-INFβIgKSAR were generated by the insertion of the Is2, SAR1, SAR2, cHS4_650, cHS4_Extended, SAR1, INFβSAR, and INFβIgKSAR elements into the unique KpnI site (outside) of the LOP-eGFP plasmid, respectively.

Viral production and titration

Using 10-cm dishes, 4–5 x 10^6 HEK293T (90% of confluency) were transfected with 10 μg of the plasmid of interest, 7 μg of pCMV_R8.91, and 3 μg of pMD2.G using 80 μg of polyethylenimine (PEI). DNA and PEI were mixed in DMEM without serum and incubated for 20 min at room temperature before being added drop-by-drop to the cells. Media was exchanged 5 h post-transfection, and supernatants were harvested at 48 h and 72 h after transfection and filtered through a 0.45-μm filter (Nalgene, Rochester, NY), aliquoted, and stored at −80°C. Inducible vectors were concentrated by ultracentrifugation at 90000 g during 2 h at 4°C min with a Sorvall centrifuge and resuspended in TexMACs media for primary T cells or DMEM media for other cells prior aliquot and storage at −80°C.

Briefly, for the estimation of the efficient viral titer, 10^5 cells were incubated with different volume of viral supernatant. Percentage of eGFP+ cells was determined by flow cytometry 72 h post-transduction in the presence of Dox, and transducing units per ml (TU/ml) were estimated according to the formula:

$$Titer = \frac{100,000\ plated\ cells \times \%GFP + cells \times 1,000}{microliters\ of\ LVs\ used}$$

Cell transduction

Briefly, 10^5 cells of Jurkat, K562, Namalwa, or Nalm6 were incubated with different volumes of viral supernatants during 4.5 h post-spinoculation (30 min at 32°C, 800 g) in order to achieve similar percentage of transduction. 10^5 cells MiaPaCa2, HEK-293T cells, or SK-MES-1 were plated with viral supernatants in a 24-well-plate, and after 5 h, medium was exchanged. For T cell transduction, T cells were incubated with LVs in a 150-mL falcon-tube and spinoculated at 800 g for 1 h at 32°C. After 5 h, cells were washed and plated at a density of 10^6 c/ml. Cell transduction was evaluated by flow cytometry.

Protransduzin-mediated transduction of primary T cells

T cells were activated with TransAct (Miltenyi Biotec) as previously described for 48 h and then washed with PBS prior to transduction. Protranduzin (PTD, JPT Peptide Technologies) was prepared following manufacturer's instructions to obtain a concentration of 10 mg/mL. Then, PTD was gently dissolved in PBS (1 mg/mL) and allowed for the fibril's formation for 10 min at RT. After that, different concentrations of PTD (12.5, 25, 50 μg/mL) were added to the viral supernatant and incubated for 5 min at RT. 50 μL of a cell suspension at 1×107 cells/ml was inoculated to obtain a final volume of 250 μL for a 48-well-plate. T cells were spinoculated at 800 g for 1 h at 32°C. After 5 h, cells were washed and seeded at 1×10^6 cells/ml and cultured with TexMACs supplemented with 10 ng/mL of IL-7 and IL-15 (Miltenyi Biotec) and 1% P/S (Biowest)

Clonal SK-MES pri-Let7a cell line generation

To generate clonal cell lines, cells were diluted and seeded in 96-well plates at 0.5 cells/well. Fresh medium was added a week after seeding. Around 14 days after seeding, positive wells (i.e., those with a single colony of cells) were passed to a 48-well plate. Clonal cell lines were subsequently expanded until they reached 100% confluency in a 24-well plate, and then they were detached with trypsin, and 80% was used for freezing, while 20% was pelleted for gDNA extraction. Selection of positive clones was analyzed by PCR. Briefly, PCRs were performed with 60 ng of gDNA using KAPA2G Fast HotstartReadyMix PCR Kit (Kapa Biosystems) following the manufacturer's instructions and run in a 1% agarose gel. The primers used map to the LTR region of the lentivirus in a way that ensures that amplification can only occur upon viral integration ΔU3-LTR-Fw (GATCTGCTTTTTGCTTGTACT) and PBS-LTR-Rv (GAGTCC TGCGTCGAGAGAGC).

Doxycycline and tetracycline

Doxycycline hyclate and tetracycline (Sigma-Aldrich) were dissolved in cell culture water, sterilized though 0.1-μm filtering (Millipore), and aliquoted at 10 μg/mL for storage at −20°C. Once thawed,

aliquots were maintained at 4°C for a maximum of 7 days. For oral administering, Dox was added to strawberry jelly (preparation for children) dissolved in warm sterile water and let to solidify at 4°C.

Inducibility calculation

The inducibility formula considers the percentage, median of intensity, and leaking (expression in the absence of Dox), as depicted in Figure S1A. Non-transduced (NT) cells in the background were subtracted:

$$Inducibility =$$

$$\frac{\%GFP\ positive\ cells\ (+Dox)\ x\ MeFI\ of\ eGFP\ positive\ gate\ (+Dox)}{\%eGFP\ positive\ cells\ (-Dox)\ x\ MeFI\ of\ total\ population\ (-Dox)}$$

Applying this formula, we can obtain values that represent the ability of the vector to induce transgene expression in the presence of Dox (ON state) while keeping it silenced in its absence (OFF state) on the bulk transduced population. We use the MFIe of the GFP+ cells (+Dox), instead of the MFI of the total population, to take into account only those cells that have been genetically modified. There are alternative formulas available to measure inducibility that could also be used. For instance, we considered a formula that is similar to the one used, but it used the MeFI of eGFP positive gate (–Dox) instead of the MeFI of total population (–Dox). However, using this formula, we encountered difficulties in obtaining consistent inducibility values for LOP LVs across different cell types and even within the same cell line with varying transduction efficiencies. The reason for the observed variability was that the formula imposed excessive penalties on the inducibility values when a small number of cells with high MFI for eGFP were present. This penalization had a particularly strong effect when the transduction efficiency was low, resulting in inconsistent inducibility values.

Flow cytometry

T cells were stained with anti-hCD45RA-PE (1:400) or anti-hCD45RA.FITC (1:400), anti-hCD62L-PE-Cy7 (1:400), and anti-hCD3-PerCP-Cy5 (1:400) (all from eBioscience-Invitrogen) during 30 min on ice. CAR expression was measured indirectly by the surface expression of truncated EGFR with anti-hEGFR-PE (Biolegend, 1:100). Then, cells were washed with PBS at 400 g for 5 min. Fluorescence was immediately acquired in a FACSCantoII cytometer, and data were analyzed with FlowJo v10 (TreeStart).

In the case of humanized murine samples, cells were washed with cold PBS + 2% BSA + 2 mM EDTA ("FACS buffer") and incubated with anti-murine CD16/CD32 (Thermo Fisher, 1:100), human FcR blocking (Miltenyi, 1:00), and 5% of mouse serum for 20 min on ice. After one wash with FACs buffer, cells were stained with anti-human CD3-PerCP-Cy5.5 (1:200) for Jurkat-mice model or with anti-human CD19-APC (1:200, eBiosciences) for Namalwa mice model during 30 min on ice and dark for 30 min. Cells were fixed with fresh PFA (2%) prior to acquisition.

Cytotoxicity assays

Target cells (CD19+), such as Namalwa and Nalm-6 cells expressing eGFP-Nanoluc, and non-target cells (CD19–) K562 cells were co-cultured at 5×10^3 cells per well in 96-well U-bottom plates and incubated with T cells at a ratio of 1:1 (Target cells:T cells expressing a 15%–20% CAR+ cells) in non-supplemented TexMACS during 48 h.

In vivo animal models and bioluminescence analysis

Jurkat and Namalwa cells transduced with inducible vectors were inoculated intravenously into NSG (Jackson Laboratory, #RRID:IMSR_JAX:00555) at a ratio of 1×10^6 cells and 0.2×10^6 cells, respectively. Dox was orally administered dissolved in jelly and provided twice a week for *ad libitum* uptake. For bioluminescence analysis, furimazine (Nano-Glo, Promega) was dissolved at 1/60 in PBS and injected intraperitoneally immediately prior to acquisition on an IVIS analyzer (PerkinElmer) during 180 s, open field. Images were analyzed using the Living Image 3.2 (PerkinElmer) or AURA Imaging Software 3.2 (Spectral Instruments Imaging). Mice were sacrificed after experiencing a weight loss higher than 20%. BM samples were obtained by the perfusion of both femurs and tibias, and cells were filtered through a 40-µm cell strainer.

For *in vivo* analysis of LOP-Is2 primary T cells, freshly isolated T cells were independently transduced with LOPIs2 or LOPIs2-CAR, and after 5 h, cells were transferred to a G-Rex 24 plate (ScaleReady) at a density of 1×10^6 per cm^2 and cultured with TexMACS supplemented with 10 ng/ml of IL-7 and IL-15 and 1% P/S for 6 days in the absence of Dox. Samples were induced with Dox to determine the percentage of transduction, obtaining a 23% of LOP+ and 20% of iCAR+ transduced cells.

For CAR experiments, 2.5×10^3 Namalwa GFP-Nluc cells (described in Tristán-Manzano et al.[59] and Maldonado et al. 2022[67]) were inoculated via tail injection in female NSG mice, 2 days prior to T cells inoculation. Intravenous infusion of T cells (a mixture of LOP and iCAR+ cells) was performed into N(-Dox) = 4; N(+Dox) = 4, with the total number of NT T cells as control in N(non-transduced) = 3 mice. Immediately before inoculation, 10 ng/ml of Dox was added to the T cells of +Dox mice. Dox-treated mice were orally supplemented with 500 ng/ml of Dox dissolved in water. At day 4 post-T infusion, animals were bleeding from the vein tail, and CAR expression was analyzed in hCD3+ cells present in the blood through tEGR staining. For a reversion experiment at day 11 post-T infusion, one mouse from –Dox group was supplemented with Dox, and two mice from the +Dox group were separated, and no more Dox was supplied. Reversion groups were as follows: NT(3); –Dox (3); +Dox (3); Reversion, R(2). eGFP and CAR expressions were measured in hCD3+ gate from BM, spleen, and liver. Brain and blood were also analyzed, but significant human CD3+ populations were not found at the day of the sacrifice.

Vector copy number analysis by qPCR

To analyze the copy number, we used 60 ng of gDNA in the first well and then four 1/10 serial dilutions. Primers used to quantify the

number of integrated copies were "ΔU3-LTR-Fw" and "PBS-LTR-Rv"). Albumin was used to normalize (hAlb-Fw: GCTGTCATCT CTTGTGGGCTGT and hAlb-Rev: ACTCATGGGAGCTGCTGGT TC). We used KAPA SYBR FAST Universal qPCR (KAPA Biosystems) in a program (95°C × 3′ + 60°C × 30′) × 40 cycles + (95°C × 1′ + 55°C × 30′ + 95°C × 30′) Mx3005P QPCR System from Stratagene (Agilent Technologies, Santa Clara, CA, USA). Quantification was performed by comparison with a control cell line that contains one integrated copy per cell (previously generated in the lab). We estimated that 60 ng corresponds to ∼10,000 cells, therefore to 10,000 copies.

Statistical analysis
Statistical analysis was performed using GraphPad Prism 9.0.2 software (GraphPad Software, La Jolla, CA). Data were expressed as the mean ± SEM. Performed statistical tests were indicated for each experiment.

DATA AVAILABILITY
Data supporting the figures generated are available from the authors under written demand.

SUPPLEMENTAL INFORMATION
Supplemental information can be found online at https://doi.org/10.1016/j.omtn.2023.03.018.

DECLARATION OF INTERESTS
F.M., P.M., and K.B. are inventors of the patents entitled "Highly Inducible Dual-Promoter Lentiviral Tet-On System" (PCT/EP2012/059408), "Lent-on-plus system for conditional expression in human stem cells" (PCT/EP2017/078246), and "Insulator to improve gene transfer vectors" (PCT/EP2014/055027). M.T.M., P.J.L., and C.B.B. were employed by LentiStem Biotech.

REFERENCES

1. Iglesias-Lopez, C., Agustí, A., Vallano, A., and Obach, M. (2021). Current landscape of clinical development and approval of advanced therapies. Mol. Ther. Methods Clin. Dev. 23, 606–618.

2. Park, S., Pascua, E., Lindquist, K.C., Kimberlin, C., Deng, X., Mak, Y.S.L., Melton, Z., Johnson, T.O., Lin, R., Boldajipour, B., et al. (2021). Direct control of CAR T cells through small molecule-regulated antibodies. Nat. Commun. 12, 710.

3. June, C.H. (2016). Remote controlled CARs: towards a safer therapy for leukemia. Cancer Immunol. Res. 4, 643.

4. Sakemura, R., Terakura, S., Watanabe, K., Julamanee, J., Takagi, E., Miyao, K., Koyama, D., Goto, T., Hanajiri, R., Nishida, T., et al. (2016). A tet-on inducible system for controlling CD19-chimeric antigen receptor expression upon drug administration. Cancer Immunol. Res. 4, 658–668.

5. Brandt, L.J.B., Barnkob, M.B., Michaels, Y.S., Heiselberg, J., and Barington, T. (2020). Emerging approaches for regulation and control of CAR T cells: a mini review. Front. Immunol. 11, 326.

6. Tristán-Manzano, M., Justicia-Lirio, P., Maldonado-Pérez, N., Cortijo-Gutiérrez, M., Benabdellah, K., and Martin, F. (2020). Externally-controlled systems for immunotherapy: from bench to bedside. Front. Immunol. 11, 2044.

7. Eggers, R., de Winter, F., Hoyng, S.A., Hoeben, R.C., Malessy, M.J.A., Tannemaat, M.R., and Verhaagen, J. (2019). Timed GDNF gene therapy using an immune-evasive gene switch promotes long distance axon regeneration. Brain 142, 295–311.

8. Le Guiner, C., Stieger, K., Toromanoff, A., Guilbaud, M., Mendes-Madeira, A., Devaux, M., Guigand, L., Cherel, Y., Moullier, P., Rolling, F., and Adjali, O. (2014). Transgene regulation using the tetracycline-inducible TetR-KRAB system after AAV-mediated gene transfer in rodents and nonhuman primates. PLoS One 9, e102538.

9. Gu, X., He, D., Li, C., Wang, H., and Yang, G. (2018). Development of inducible CD19-CAR T cells with a tet-on system for controlled activity and enhanced clinical safety. Int. J. Mol. Sci. 19, 3455.

10. No, D., Yao, T.P., and Evans, R.M. (1996). Ecdysone-inducible gene expression in mammalian cells and transgenic mice. Proc. Natl. Acad. Sci. USA 93, 3346–3351.

11. Karns, L.R., Kisielewski, A., Gulding, K.M., Seraj, J.M., and Theodorescu, D. (2001). Manipulation of gene expression by an ecdysone-inducible gene switch in tumor xenografts. BMC Biotechnol. *1*, 11.

12. Cheng, S., van Gaalen, M.M., Bähr, M., Garea-Rodriguez, E., and Kügler, S. (2021). Optimized pharmacological control over the AAV-Gene-Switch vector for regulable gene therapy. Mol. Ther. Methods Clin. Dev. *23*, 1–10.

13. Maddalena, A., Tereshchenko, J., Bähr, M., and Kügler, S. (2013). Adeno-associated virus-mediated, mifepristone-regulated transgene expression in the brain. Mol. Ther. Nucleic Acids *2*, e106.

14. Liefhebber, J.M., Martier, R., Van der Zon, T., Keskin, S., Huseinovic, A., Lubelski, J., Blits, B., Petry, H., and Konstantinova, P. (2019). In-depth characterization of a mifepristone-regulated expression system for AAV5-mediated gene therapy in the liver. Mol. Ther. Methods Clin. Dev. *13*, 512–525.

15. Hjelm, B.E., Grunseich, C., Gowing, G., Avalos, P., Tian, J., Shelley, B.C., Mooney, M., Narwani, K., Shi, Y., Svendsen, C.N., et al. (2016). Mifepristone-inducible transgene expression in neural progenitor cells in vitro and in vivo. Gene Ther. *23*, 424–437.

16. Qian, C., Liu, X.Y., and Prieto, J. (2006). Therapy of cancer by cytokines mediated by gene therapy approach. Cell Res. *16*, 182–188.

17. Cheng, S., Tereshchenko, J., Zimmer, V., Vachey, G., Pythoud, C., Rey, M., Liefhebber, J., Raina, A., Streit, F., Mazur, A., et al. (2018). Therapeutic efficacy of regulable GDNF expression for Huntington's and Parkinson's disease by a high-induction, background-free "GeneSwitch" vector. Exp. Neurol. *309*, 79–90.

18. Zhou, X., Dotti, G., Krance, R.A., Martinez, C.A., Naik, S., Kamble, R.T., Durett, A.G., Dakhova, O., Savoldo, B., Di Stasi, A., et al. (2015). Inducible caspase-9 suicide gene controls adverse effects from alloreplete T cells after haploidentical stem cell transplantation. Blood *125*, 4103–4113.

19. Stavrou, M., Philip, B., Traynor-White, C., Davis, C.G., Onuoha, S., Cordoba, S., Thomas, S., and Pule, M. (2018). A rapamycin-activated caspase 9-based suicide gene. Mol. Ther. *26*, 1266–1276.

20. Gossen, M., and Bujard, H. (1992). Tight control of gene expression in mammalian cells by tetracycline-responsive promoters. Proc. Natl. Acad. Sci. USA *89*, 5547–5551.

21. Chao, J.S., Chao, C.C., Chang, C.L., Chiu, Y.R., and Yuan, C.J. (2012). Development of single-vector Tet-on inducible systems with high sensitivity to doxycycline. Mol. Biotechnol. *51*, 240–246.

22. Urlinger, S., Baron, U., Thellmann, M., Hasan, M.T., Bujard, H., and Hillen, W. (2000). Exploring the sequence space for tetracycline-dependent transcriptional activators: novel mutations yield expanded range and sensitivity. Proc. Natl. Acad. Sci. USA *97*, 7963–7968.

23. Toniatti, C., Bujard, H., Cortese, R., and Ciliberto, G. (2004). Gene therapy progress and prospects: transcription regulatory systems. Gene Ther. *11*, 649–657.

24. Morimoto, M., and Kopan, R. (2009). rtTA toxicity limits the usefulness of the SP-C-rtTA transgenic mouse. Dev. Biol. *325*, 171–178.

25. Perl, A.K., Zhang, L., and Whitsett, J.A. (2009). Conditional expression of genes in the respiratory epithelium in transgenic mice: cautionary notes and toward building a better mouse trap. Am. J. Respir. Cell Mol. Biol. *40*, 1–3.

26. Whitsett, J.A., and Perl, A.K.T. (2006). Conditional control of gene expression in the respiratory epithelium: a cautionary note. Am. J. Respir. Cell Mol. Biol. *34*, 519–520.

27. Sisson, T.H., Hansen, J.M., Shah, M., Hanson, K.E., Du, M., Ling, T., Simon, R.H., and Christensen, P.J. (2006). Expression of the reverse tetracycline-transactivator gene causes emphysema-like changes in mice. Am. J. Respir. Cell Mol. Biol. *34*, 552–560.

28. Schmitt, A., Schulze-Osthoff, K., and Hailfinger, S. (2018). Correspondence: T cells are compromised in tetracycline transactivator transgenic mice. Cell Death Differ. *25*, 634–636.

29. Yao, F., Svensjö, T., Winkler, T., Lu, M., Eriksson, C., and Eriksson, E. (1998). Tetracycline repressor, tetR, rather than the tetR-mammalian cell transcription factor fusion derivatives, regulates inducible gene expression in mammalian cells. Hum. Gene Ther. *9*, 1939–1950.

30. Yao, F., Theopold, C., Hoeller, D., Bleiziffer, O., and Lu, Z. (2006). Highly efficient regulation of gene expression by tetracycline in a replication-defective herpes simplex viral vector. Mol. Ther. *13*, 1133–1141.

31. Trapani, J.G., and Korn, S.J. (2003). Control of ion channel expression for patch clamp recordings using an inducible expression system in mammalian cell lines. BMC Neurosci. *4*, 15.

32. Reeves, P.J., Callewaert, N., Contreras, R., and Khorana, H.G. (2002). Structure and function in rhodopsin: high-level expression of rhodopsin with restricted and homogeneous N-glycosylation by a tetracycline-inducible N-acetylglucosaminyltransferase I-negative HEK293S stable mammalian cell line. Proc. Natl. Acad. Sci. USA *99*, 13419–13424.

33. Wiederschain, D., Wee, S., Chen, L., Loo, A., Yang, G., Huang, A., Chen, Y., Caponigro, G., Yao, Y.M., Lengauer, C., et al. (2009). Single-vector inducible lentiviral RNAi system for oncology target validation. Cell Cycle *8*, 498–504.

34. Ogueta, S.B., Yao, F., and Marasco, W.A. (2001). Design and in vitro characterization of a single regulatory module for efficient control of gene expression in both plasmid DNA and a self-inactivating lentiviral vector. Mol. Med. *7*, 569–579.

35. Benabdellah, K., Cobo, M., Muñoz, P., Toscano, M.G., and Martin, F. (2011). Development of an all-in-one lentiviral vector system based on the original TetR for the easy generation of Tet-ON cell lines. PLoS One *6*, e23734.

36. Benabdellah, K., Gutierrez-Guerrero, A., Cobo, M., Muñoz, P., and Martín, F. (2014). A chimeric HS4-SAR insulator (IS2) that prevents silencing and enhances expression of lentiviral vectors in pluripotent stem cells. PLoS One *9*, e84268.

37. Benabdellah, K., Muñoz, P., Cobo, M., Gutierrez-Guerrero, A., Sánchez-Hernández, S., Garcia-Perez, A., Anderson, P., Carrillo-Gálvez, A.B., Toscano, M.G., and Martin, F. (2016). Lent-On-Plus Lentiviral vectors for conditional expression in human stem cells. Sci. Rep. *6*, 37289.

38. Sánchez-Hernández, S., Gutierrez-Guerrero, A., Martín-Guerra, R., Cortijo-Gutierrez, M., Tristán-Manzano, M., Rodriguez-Perales, S., Sanchez, L., Garcia-Perez, J.L., Chato-Astrain, J., Fernandez-Valades, R., et al. (2018). The IS2 element improves transcription efficiency of integration-deficient lentiviral vector episomes. Mol. Ther. Nucleic Acids *13*, 16–28.

39. Urbinati, F., Arumugam, P., Higashimoto, T., Perumbeti, A., Mitts, K., Xia, P., and Malik, P. (2009). Mechanism of reduction in titers from lentivirus vectors carrying large inserts in the 3'LTR. Mol. Ther. *17*, 1527–1536.

40. Arumugam, P.I., Urbinati, F., Velu, C.S., Higashimoto, T., Grimes, H.L., and Malik, P. (2009). The 3' region of the chicken hypersensitive site-4 insulator has properties similar to its core and is required for full insulator activity. PLoS One *4*, e6995.

41. Aker, M., Tubb, J., Groth, A.C., Bukovsky, A.A., Bell, A.C., Felsenfeld, G., Kiem, H.P., Stamatoyannopoulos, G., and Emery, D.W. (2007). Extended core sequences from the cHS4 insulator are necessary for protecting retroviral vectors from silencing position effects. Hum. Gene Ther. *18*, 333–343.

42. Rhim, T., Lee, D.Y., and Lee, M. (2013). Hypoxia as a target for tissue specific gene therapy. J. Control. Release *172*, 484–494.

43. Andreou, T., Rippaus, N., Wronski, K., Williams, J., Taggart, D., Cherqui, S., Sunderland, A., Kartika, Y.D., Egnuni, T., Brownlie, R.J., et al. (2020). Hematopoietic stem cell gene therapy for brain metastases using myeloid cell-specific gene promoters. J. Natl. Cancer Inst. *112*, 617–627.

44. Erendor, F., Eksi, Y.E., Sahin, E.O., Balci, M.K., Griffith, T.S., and Sanlioglu, S. (2021). Lentivirus mediated pancreatic beta-cell-specific insulin gene therapy for STZ-induced diabetes. Mol. Ther. *29*, 149–161.

45. Martín, F., Toscano, M.G., Blundell, M., Frecha, C., Srivastava, G.K., Santamaría, M., Thrasher, A.J., and Molina, I.J. (2005). Lentiviral vectors transcriptionally targeted to hematopoietic cells by WASP gene proximal promoter sequences. Gene Ther. *12*, 715–723.

46. Romero, Z., Toscano, M.G., Unciti, J.D., Molina, I., and Martín, F. (2009). Safer vectors for gene therapy of primary immunodeficiencies. Curr. Gene Ther. *9*, 291–305.

47. Romero, Z., Torres, S., Cobo, M., Muñoz, P., Unciti, J.D., Martín, F., and Molina, I.J. (2011). A tissue-specific, activation-inducible, lentiviral vector regulated by human CD40L proximal promoter sequences. Gene Ther. *18*, 364–371.

48. Martínez-García, J., Molina, M., Odriozola, L., Molina, A., González-Aseguinolaza, G., Weber, N.D., and Smerdou, C. (2022). A minimal bile salt excretory pump promoter allows bile acid-driven physiological regulation of transgene expression from a gene therapy vector. Cell Biosci. *12*, 79.

49. Das, A.T., Tenenbaum, L., and Berkhout, B. (2016). Tet-on systems for doxycycline-inducible gene expression. Curr. Gene Ther. *16*, 156–167.

50. Abbott, R.C., Hughes-Parry, H.E., and Jenkins, M.R. (2022). To go or not to go? Biological logic gating engineered T cells. J. Immunother. Cancer *10*, e004185.

51. Di Stasi, A., Tey, S.K., Dotti, G., Fujita, Y., Kennedy-Nasser, A., Martinez, C., Straathof, K., Liu, E., Durett, A.G., Grilley, B., et al. (2011). Inducible apoptosis as a safety switch for adoptive cell therapy. N. Engl. J. Med. *365*, 1673–1683.

52. Lee, S.M., Kang, C.H., Choi, S.U., Kim, Y., Hwang, J.Y., Jeong, H.G., and Park, C.H. (2020). A chemical switch system to modulate chimeric antigen receptor T cell activity through proteolysis-targeting chimaera technology. ACS Synth. Biol. *9*, 987–992.

53. Lajoie, M.J., Boyken, S.E., Salter, A.I., Bruffey, J., Rajan, A., Langan, R.A., Olshefsky, A., Muhunthan, V., Bick, M.J., Gewe, M., et al. (2020). Designed protein logic to target cells with precise combinations of surface antigens. Science *369*, 1637–1643.

54. Roybal, K.T., Rupp, L.J., Morsut, L., Walker, W.J., McNally, K.A., Park, J.S., and Lim, W.A. (2016). Precision tumor recognition by T cells with combinatorial antigen-sensing circuits. Cell *164*, 770–779.

55. Morsut, L., Roybal, K.T., Xiong, X., Gordley, R.M., Coyle, S.M., Thomson, M., and Lim, W.A. (2016). Engineering customized cell sensing and response behaviors using synthetic notch receptors. Cell *164*, 780–791.

56. Drent, E., Poels, R., Mulders, M.J., van de Donk, N.W.C.J., Themeli, M., Lokhorst, H.M., and Mutis, T. (2018). Feasibility of controlling CD38-CAR T cell activity with a Tet-on inducible CAR design. PLoS One *13*, e0197349.

57. Xu, X., Sun, Q., Liang, X., Chen, Z., Zhang, X., Zhou, X., Li, M., Tu, H., Liu, Y., Tu, S., and Li, Y. (2019). Mechanisms of relapse after CD19 CAR T-cell therapy for acute lymphoblastic leukemia and its prevention and treatment strategies. Front. Immunol. *10*, 2664.

58. Zhang, R.Y., Wei, D., Liu, Z.K., Yong, Y.L., Wei, W., Zhang, Z.Y., Lv, J.J., Zhang, Z., Chen, Z.N., and Bian, H. (2019). Doxycycline inducible chimeric antigen receptor T cells targeting CD147 for hepatocellular carcinoma therapy. Front. Cell Dev. Biol. *7*, 233.

59. Tristán-Manzano, M., Maldonado-Pérez, N., Justicia-Lirio, P., Muñoz, P., Cortijo-Gutiérrez, M., Pavlovic, K., Jiménez-Moreno, R., Nogueras, S., Carmona, M.D., Sánchez-Hernández, S., et al. (2022). Physiological lentiviral vectors for the generation of improved CAR-T cells. Mol. Ther. Oncolytics *25*, 335–349.

60. Latta-Mahieu, M., Rolland, M., Caillet, C., Wang, M., Kennel, P., Mahfouz, I., Loquet, I., Dedieu, J.F., Mahfoudi, A., Trannoy, E., and Thuillier, V. (2002). Gene transfer of a chimeric trans-activator is immunogenic and results in short-lived transgene expression. Hum. Gene Ther. *13*, 1611–1620.

61. Ginhoux, F., Turbant, S., Gross, D.A., Poupiot, J., Marais, T., Lone, Y., Lemonnier, F.A., Firat, H., Perez, N., Danos, O., and Davoust, J. (2004). HLA-A*0201-restricted cytolytic responses to the rtTA transactivator dominant and cryptic epitopes compromise transgene expression induced by the tetracycline on system. Mol. Ther. *10*, 279–289.

62. Sack, B.K., Herzog, R.W., Terhorst, C., and Markusic, D.M. (2014). Development of gene transfer for induction of antigen-specific tolerance. Mol. Ther. Methods Clin. Dev. *1*, 14013.

63. Mautner, J., Pich, D., Nimmerjahn, F., Milosevic, S., Adhikary, D., Christoph, H., Witter, K., Bornkamm, G.W., Hammerschmidt, W., and Behrends, U. (2004). Epstein-Barr virus nuclear antigen 1 evades direct immune recognition by CD4+ T helper cells. Eur. J. Immunol. *34*, 2500–2509.

64. De Winter, F., Quijorna, I.F., Burnside, E., Hobo, B., Eggers, R., Hoyng, S.A., Mulder, H.P., Hoeben, R.C., Muir, E.M., Bradbury, E.J., and Verhaagen, J. (2022). Characterization of an immune-evading doxycycline-inducible lentiviral vector for gene therapy in the spinal cord. Exp. Neurol. *355*, 114120.

65. Chait, R., Palmer, A.C., Yelin, I., and Kishony, R. (2016). Pervasive selection for and against antibiotic resistance in inhomogeneous multistress environments. Nat. Commun. *7*, 10333.

66. Ahler, E., Sullivan, W.J., Cass, A., Braas, D., York, A.G., Bensinger, S.J., Graeber, T.G., and Christofk, H.R. (2013). Doxycycline alters metabolism and proliferation of human cell lines. PLoS One *8*, e64561.

67. Maldonado-Pérez, N., Tristán-Manzano, M., Justicia-Lirio, P., Martínez-Planes, E., Muñoz, P., Pavlovic, K., Cortijo-Gutiérrez, M., Blanco-Benítez, C., Castella, M., Juan, M., et al. (2022). Efficacy and safety of universal (TCRKO) ARI-0001 CAR-T cells for the treatment of B-cell lymphoma. Front. Immunol. *13*, 1011858.